

1

Structure and Properties of Liquids

A solution is a homogeneous mixture of physically combined two or more substances, which may be gaseous, liquid, or solid. A solution exhibits the same properties throughout its volume. The component that is present in excess is usually referred to as the solvent, whereas the other component combining with the former in different proportions is termed the solute. Under normal temperature and pressure conditions, solid NaCl, for example, dissolves in water forming its aqueous solution. Here, the solvent water is in the liquid state and is molten form of ice with its melting point $T_m = 0^\circ\text{C}$. It is a common solvent used in solutions of numerous compounds for their crystallization and purification. Similarly, compounds like NaCl, which are present in the solid state under normal temperature and pressure conditions, exist in the liquid state above their melting point T_m and serve as solvents in high-temperature solution growth.

In this chapter, general features of the structure and properties of solvents and solutions are briefly described. For more information on the topics discussed here, the reader is referred to the literature (for example, see: Atkins, 1998; Bockris and Reddy, 1970; Eggers et al., 1964; Horvath, 1985; Mortimore, 2008; Stokes and Mills, 1965; Wright, 2007).

1.1 Different States of Matter

Under appropriate temperature and pressure conditions all elements and compounds can exist in vapor, liquid, and solid states. These states are characterized by the mean distance between the atoms and molecules composing them, and the ratio of the average potential energy of atoms/molecules to their kinetic energy is a characteristic parameter of the state. In the vapor state the atoms/molecules move randomly undergoing elastic collisions among themselves in the entire space available to them and the average distance between them is much larger than their size. The attractive forces between

Nucleation and Crystal Growth: Metastability of Solutions and Melts, First Edition.
Keshra Sangwal.

© 2018 John Wiley & Sons, Inc. Published 2018 by John Wiley & Sons, Inc.

the atoms/molecules are too small to keep them close to each other. In the liquid state, the average distance between the atoms/molecules is decreased to the extent that mutual attractive forces hold them close to each other. There is short-range order between nearest neighbors and both the number and the positions of nearest neighbors are, on an average, the same for all. However, the atoms/molecules in the liquid state have sufficient kinetic energy to jump from one position to the next. In the solid state, the distance between the neighboring atoms/molecules in the entire volume is similar to the average distance between them in the liquid state. In this case, the attractive forces are strong enough to keep them in their equilibrium positions despite their thermal motion and are of long-range order.

At a given pressure p , with an increase in temperature T , every solidified material first transforms into the liquid form at a temperature T_m , and this liquid thereafter begins to boil at temperature T_b and transforms into the vapor phase. Conversely, with a slow decrease in temperature, a material initially existing in the vapor phase condenses into the liquid phase at the temperature T_b , and the cooling of the liquid later solidifies at the temperature T_m and remains in this phase. At a given pressure p , the densities d of the solid and liquid phases decrease with increasing temperature T according to the relation:

$$d(T) = d_m - k(T - T_m), \quad (1.1)$$

where T_m is the melting point of the material, d_m is the density of the solid and the liquid at the melting temperature T_m , and k is a constant characteristic of the phase. Note that the value of the density d_m of a solid at T_m is always different from the density d_m of the molten liquid at T_m . From Eq. (1.1) one obtains the expression for the volumetric thermal expansion coefficient (also called volume thermal expansivity):

$$\alpha_V = \frac{k}{d_m} = -\frac{d - d_m}{d_m(T - T_m)} = -\frac{1}{d_m} \left(\frac{\Delta d}{\Delta T} \right), \quad (1.2)$$

where the density difference is $\Delta d = (d - d_m)$ and the temperature difference is $\Delta T = (T - T_m)$. If m is the mass of the solid or liquid material of volume V , using the definition of density $d = m/V$, $dd/dV = -m/V^2$, and the differential form of Eq. (1.2) rewritten in the form

$$\alpha_V = -\frac{1}{d} \left(\frac{dd}{dT} \right) = -\frac{1}{d} \left(\frac{dd}{dV} \right)_p \left(\frac{dV}{dT} \right)_p = \frac{V}{m} \left(-\frac{m}{V^2} \right) \left(\frac{dV}{dT} \right) = \frac{1}{V} \left(\frac{dV}{dT} \right), \quad (1.3)$$

one obtains

$$\frac{\Delta V}{V_0} = \alpha_V \Delta T. \quad (1.4)$$

where V and dV are the volume and the change in the volume, respectively, of the solid and the liquid. According to Eq. (1.4), the volume V of a solid and a liquid increases linearly with an increase in temperature T in contrast to Eq. (1.1), which predicts that their density d decreases linearly with increasing T .

The physical properties of liquids differ from those of solids. For example, melting of solids leads to an increase in their volume insignificantly (about 10%). Consequently, the average distance between their atoms/molecules after melting remains practically unchanged. In contrast to this, the volume thermal expansion coefficient α_V of solids is one-order lower than that in the liquid state. These differences in the physical properties of materials in the solid and liquid states are associated with differences in the nature of interactions between the atoms/molecules in the two states.

In order to compare the thermal properties of solids and liquids, it is convenient to consider their temperature dependence of the specific volume ϕ_V and the volume thermal expansion coefficient α_V . The specific volume ϕ_V , defined as inverse of density d (i.e. $\phi_V = 1/d$), is the measure of V of Eq. (1.4), whereas the thermal expansion coefficient α_V of the compound is related to density d by Eq. (1.3). Figure 1.1 illustrates the dependence of specific volume ϕ_V on temperature T of the commonly used solvent water and its solid-phase ice. From the figure it may be noted that:

- 1) At 0 °C the specific volume ϕ_V of ice is about 10% higher than that of water, and its values for ice increases linearly with temperature, with slope

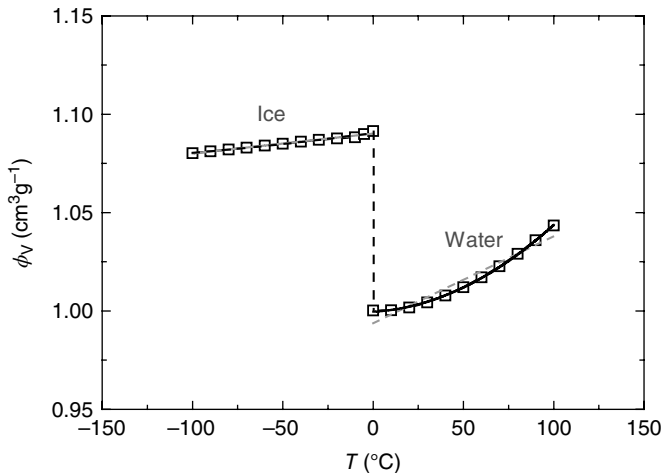


Figure 1.1 Dependence of specific volume ϕ_V on temperature T of water and ice. Data of density d for ice from www.EngineeringToolBox.com accessed 12 January 2017, and for water from Lide (1996/1997). For water solid, a curve is drawn according to Eq. (1.5), whereas the dashed curve shows a linear dependence.

$1.014 \cdot 10^{-4} \text{ cm}^3 \cdot \text{g}^{-1} \cdot \text{K}^{-1}$. Note that it is immaterial here whether the units of ϕ_V are $\text{cm}^3 \cdot \text{g}^{-1} \cdot \text{K}^{-1}$ or $\text{cm}^3 \cdot \text{g}^{-1} \cdot ^\circ\text{C}^{-1}$ because we are concerned with temperature difference ΔT .

- 2) The value of ϕ_V for water increases up to about 30°C practically linearly with temperature with a slope equal to that for ice, but beyond this temperature its value increases much rapidly practically following a second-order dependence:

$$\phi_V = \phi_{V0} + a_1(T - T_0) + a_2(T - T_0)^2, \quad (1.5)$$

where $T_0 = 273.15 \text{ K}$, $\phi_{V0} = 0.9996(\pm 0.0003) \text{ cm}^3 \cdot \text{g}^{-1}$, $a_1 = 5.441(\pm 1.347) \cdot 10^{-5} \text{ cm}^3 \cdot \text{g}^{-1} \cdot \text{K}^{-1}$, $a_2 = 3.874(\pm 0.130) \cdot 10^{-6} \text{ cm}^3 \cdot \text{g}^{-1} \cdot \text{K}^{-2}$, and T is taken in K.

The above observations are associated with the difference in the structures of ice and water. An individual water molecule is nonlinear with the H—O—H angle of about 105° and the distribution of the four pairs of electrons of the six electrons from oxygen and the two electrons from hydrogen atoms is in four approximately equivalent directions. However, the oxygen atom is not situated at the center of the tetrahedron. Thus, a water molecule may be considered an electric dipole. This property of water molecules gives an open structure to ice lattice. The ice lattice consists of oxygen atoms lying in layers with each layer forming a network structure of open hexagonal rings composed of associated water molecules (see Figure 1.2). With an increase in temperature of network water, a molecule breaks its hydrogen bonds with the network and moves into interstitial regions. Thus, in liquid water there are networks of associated water molecules as well as certain fraction of free, unassociated water molecules. With increasing temperature more free, unassociated water molecules are broken from the associated network structure such that the fraction of unassociated water molecules increases at the expense of associated water molecules of the network structure. This results in increasing specific volume ϕ_V of liquid water where its value is determined by the ice and the free, unassociated water structures in the region below and above about 25°C , respectively.

Figure 1.3 illustrates the dependence of volume thermal expansivity α_V on temperature T of ice and water. As expected from the nature of vibrations of water molecules in ice and liquid water, the expansion coefficient α_V is practically constant at $9.4 \cdot 10^{-5} \text{ K}^{-1}$ up to -30°C and then drops to the value of liquid water. For liquid water the value of α_V rapidly increases with temperature and approaches $7.5 \cdot 10^{-4} \text{ K}^{-1}$ at 100°C , following the binomial relation:

$$\alpha_V = \alpha_{V0} + \alpha_1(T - T_0) + \alpha_2(T - T_0)^2, \quad (1.6)$$

where $T_0 = 273.15 \text{ K}$, $\alpha_{V0} = -3.13(\pm 1.23) \cdot 10^{-5} \text{ K}^{-1}$, $\alpha_1 = 1.207(\pm 0.057) \cdot 10^{-5} \text{ K}^{-2}$, $\alpha_2 = -4.49(\pm 0.55) \cdot 10^{-8} \text{ K}^{-3}$, and the temperature T is taken in K. The difference in the trends of the temperature dependence of α_V of ice and liquid water is obvious and is associated with their structures.

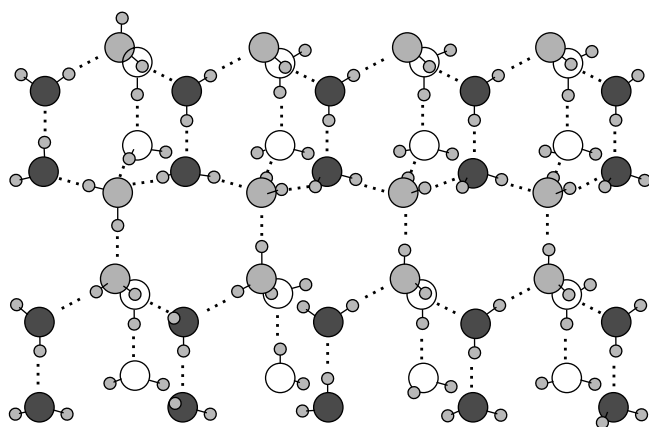


Figure 1.2 Network structure of ice with large interstitial spaces capable of free, unassociated water molecules. Structure of a free water molecule is also shown. Large and small circles denote oxygen and hydrogen atoms, respectively. Solid lines represent covalent bonds, whereas dotted lines represent hydrogen bonds. Dark, gray, and open oxygen atoms represent first, second, and third levels of water molecules parallel to the plane of the paper. Oxygen atoms lie in layers perpendicular to the plane of the paper in a direction parallel to the shorter edge (i.e. the x direction), with each layer forming a network structure of open hexagonal rings composed of water molecules joined by hydrogen bonds. Internet source of image file is unknown.

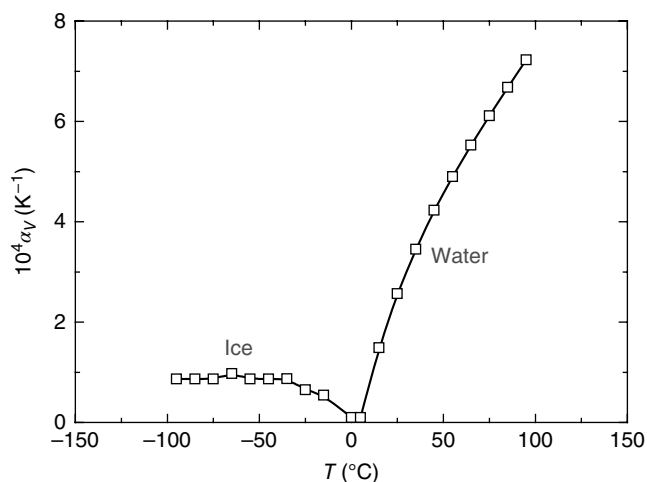


Figure 1.3 Dependence of volume thermal expansivity α_V on temperature T of water and ice. Sources of data of density d as given in Figure 1.1.

The formation of crystalline nuclei and the growth of these nuclei occur in the liquid phase. These processes of nucleation and growth are usually called crystallization processes. The liquid for crystallization can be a melt of an element or a compound itself or a solution prepared at a particular temperature by dissolving the element or the compound, called the solute, in a suitable nonreactive solvent. In this chapter, some general features of common solvents and solutions used for the crystallization of different inorganic and organic compounds are described, using typical examples of dilute, saturated, and supersaturated solutions of the compounds. Because of difficulties in finding appropriate solvents for the preparation of solutions of elements and lack of interest in their crystallization from solutions, they are not considered here.

1.2 Models of Liquid Structure

All solvents used in the preparation of solutions of different solutes for their crystallization are composed of molecules of various sizes. Some of the solvents used in crystallization from solutions of inorganic and organic compounds and their properties are listed in Table 1.1.

The simplest solvent is water composed of water molecules (molecular weight 18) while butanol, glycerol, and *N*-methyl-2-pyrrolidone (NMP), with molecular weights 74, 92, and 99, respectively, are solvents composed of relatively complex molecules. Some general trends of the different properties of these solvents may be noted:

- 1) Water has relatively high density d , high viscosity η , high dielectric constant ϵ , high melting point T_m , and high boiling point T_b than the corresponding properties of the lowest alcohols like methanol and ethanol.
- 2) Simple alcohols have roughly the same density d at 20 °C, whereas melting point T_m and dielectric constant ϵ decrease, and boiling point T_b and viscosity η increase with increasing molecular weight.
- 3) Normal alcohols like 1-propanol and 1-butanol have slightly higher density, higher dielectric constant ϵ , and higher boiling point T_b than those of iso-alcohols 2-propanol and 2-butanol. However, viscosity η and melting point T_m of normal alcohols are lower than those of iso-alcohols.
- 4) Other high carbon-containing solvents like ethylene glycol, glycerol, and NMP have high density d , high viscosity η , high dielectric constant ϵ , and relatively high melting point T_m and boiling point T_b than those of simple alcohols.

The aforementioned differences in the properties of the solvents are associated with the structure of their molecules. The structure of molecules determines not only the nature of interactions holding the molecules in the liquid

Table 1.1 Properties of some commonly used solvents.

Solvent	MW	d ($\text{g}\cdot\text{cm}^{-3}$) ^a	η ($\text{mPa}\cdot\text{s}$) ^b	ϵ (-) ^a	T_m ($^{\circ}\text{C}$)	ΔH_m ($\text{kJ}\cdot\text{mol}^{-1}$)	T_b ($^{\circ}\text{C}$)
Water (H_2O)	18.0	0.9982	0.890	80.1	0	6.01	100
Acetone ($\text{C}_2\text{H}_6\text{CO}$)	50.08	0.790	0.306	21.01	-95.0	26.53	56.3
MeOH (CH_3OH)	32.04	0.7914	0.544	33.3	-97.6	3.18	64.6
EtOH ($\text{C}_2\text{H}_5\text{OH}$)	46.07	0.7893	1.074	25.3	-114.1	5.02	78.2
1-PrOH ($\text{C}_3\text{H}_7\text{OH}$)	60.10	0.8035	1.945	20.8	-126.1	5.2	97.2
2-PrOH ($\text{C}_3\text{H}_7\text{OH}$)	60.10	0.7855	2.038	20.18	-89.5	5.37	82.3
1-BuOH ($\text{C}_4\text{H}_9\text{OH}$)	74.12	0.8098	2.544	17.84	-89.8	9.28	117.7
2-BuOH ($\text{C}_4\text{H}_9\text{OH}$)	74.12	0.8063	3.096	17.26	-114.7	—	99.5
Ethylene glycol ($\text{C}_2\text{H}_6\text{O}_2$)	62.07	1.1088	16.1	41.4	-13.0	—	197.3
Glycerol ($\text{C}_3\text{H}_8\text{O}_3$)	92.09	1.2613	18.2	46.53	18.2	8.48	290
NMP ($\text{C}_5\text{H}_9\text{NO}$)	99.13	1.0230	—	32.55	-24.0	202	—

BuOH, butanol; EtOH, ethyl alcohol; MeOH, methyl alcohol; MW, molecular weight; NMP, *N*-methyl-2pyrrolidine; PrOH, propanol. Other symbols are: density d , viscosity η , dielectric constant ϵ , boiling temperature T_b , melting temperature T_m , and enthalpy of melting ΔH_m .

^a 20 $^{\circ}\text{C}$.

^b 25 $^{\circ}\text{C}$.

state and their packing but also determines their motion in the liquid state and processes of solidification and evaporation.

Depending on the structure of molecules composing different liquids, the liquids may be classified as polar, nonpolar, and apolar. Molecules of a polar liquid are uncharged with an overall dipole moment, which may be the result of one individual polar bond within the molecule. Molecules of a nonpolar liquid are uncharged neutral with a zero dipole moment but contain bonds that are polar. Molecules of apolar liquids are neutral with an overall zero dipole moment. A measure of the polar or nonpolar nature of molecules composing a liquid is its dielectric constant ϵ (see Table 1.1).

Solidification and evaporation of liquids occur at their standard melting point T_m and boiling point T_b with corresponding changes in the heat energies ΔH_m and ΔH_b , respectively, under atmospheric pressure, and are associated with the entropy changes $\Delta H_m/T_m$ and $\Delta H_b/T_b$, respectively. At equal pressures the entropy of the phase stable at higher temperatures is always higher than that at lower temperatures. Therefore, vaporization of different liquids leads to an increase in their entropy at their normal boiling points and the value of this entropy is higher than that in solidification, i.e. $\Delta H_b/T_b > \Delta H_m/T_m$.

Vaporization entropy $\Delta H_b/T_b \approx 10.5R_G \approx 88 \text{ kJ mol}^{-1} \cdot \text{K}^{-1}$ for many organic liquids is referred to as normal liquids and the above relationship is called *Trounton's rule*. Here, the gas constant $R_G = k_B N_A$, where k_B is the Boltzmann constant and N_A is the Avogadro number. However, this vaporization entropy $\Delta H_b/T_b$ is about $5R_G$ for simple monoatomic liquids, $7.5R_G$ for acetic acid, and up to about $15R_G$ for water, alcohols, and other hydrogen-bonded liquids, and several bivalent chlorides such as PbCl_2 and ZnCl_2 , which behave as associated liquids. The trends of melting entropy $\Delta H_m/T_m$ of different substances are also similar to those of the vaporization entropy $\Delta H_b/T_b$, but their values are lower than those of $\Delta H_b/T_b$ for a given substance. For substances that behave as normal liquids, $\Delta H_m/T_m$ lies between about R_G and $2R_G$, but for associated liquids like water and bivalent chlorides, its value is up to $5R_G$. In the case of alkali halides and many organic compounds, $\Delta H_m/T_m$ is about $3R_G$ and $6R_G$, respectively (Sangwal, 1989; see Section 2.5).

There are also many organic liquids with $\Delta H_m/T_m < R_G$ but they have relatively a low number n of C atoms in their composition. Figure 1.4 shows the data of $\Delta H_m/R_G T_m$ as a function of the number n of carbon atoms in the chemical formula of some simple alcohols and alkanes, with $n \leq 5$ and $n \leq 10$, respectively. If the data for methane, butane, and nonane are excluded, the data for alkanes may be represented by the relation:

$$\frac{\Delta H_m}{R_G T_m} = 0.08 + 0.085n. \quad (1.7)$$

Except for pentanol, 2-propanol, and glycerol, the data for alcohols also follow this relation. The above relation holds for linear alcohols and alkanes, and deviations may be attributed to errors in the data and nonlinear nature of their chains. The linear dependence of $\Delta H_m/R_G T_m$ on the carbon number n of alkanes and alcohols suggests that, starting from methane and methanol, the melting entropy of these liquids is additive with entropy increment $(\Delta H_m/T_m)/n = 0.085R_G$ and energy increment $\Delta H_m/n = 0.085R_G T_m$ per CH_2 - group. A constant $\Delta H_m/R_G T_m = 6$ for organic compounds suggests that melting of organic compounds involves strong association of their molecules.

In order to understand different properties of solvents, following the models for molten liquid electrolytes, discussed by Bockris and Reddy (1970), different models may be considered. Since a liquid can be obtained either by melting its

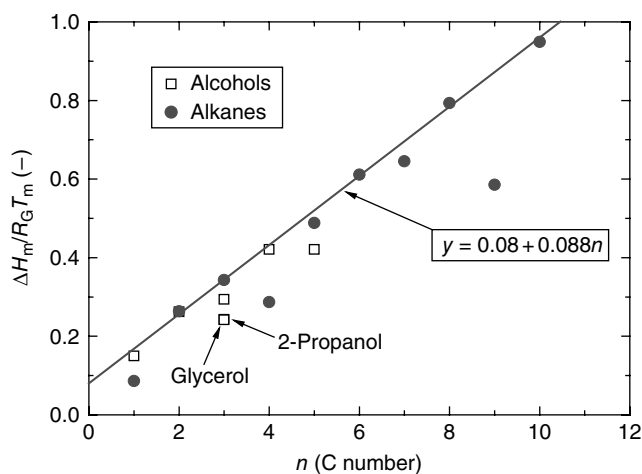


Figure 1.4 Relationship between $\Delta H_m/R_G T_m$ and number n of carbon atoms in the chemical formula of some simple alcohols and alkanes. Linear plot represents data according to relation (1.7). Source: Original data from Lide (1996/1997).

crystalline solid or by cooling its vapor, there are two ways of looking at the models of liquids. Thus, there are *lattice-based* and *gas-based models* for a liquid. The main observation that a model should explain is an increase in the volume upon melting and roughly the same distance between the molecules in the crystalline and liquid phases. The volume increase without a change in the mean distance between the neighboring molecules suggests that melting of the crystalline solid introduces empty space into the liquid. It is the mode of description of this empty space that differentiates one model from another.

The simplest model of a liquid is based on the concept of injection of vacancies known as Schottky defects in a crystalline lattice. Vacancies are produced in the lattice by removal of atoms/molecules from lattice sites in the interior to the crystal surface (Figure 1.5a). Vacancies are produced randomly inside the crystal with simultaneous volume increase through displacement of removed atoms/molecules from lattice sites to the crystal surface. As the temperature of the solid is increased, the number of vacancies increases as a result of the thermal motion of atoms/molecules of lattice sites and at the melting point they are so numerous in the lattice that the long-range order disappears. The vacancies are roughly of the size of displaced atoms/molecules. Since vacancies are produced at lattice sites, one refers to the *quasi-lattice model*.

When numerous vacancies are introduced in the crystalline lattice, the definition of crystalline lattice as a three-dimensional array of points no longer holds. Now, atoms/molecules and vacancies of the molten system may be considered to be distributed randomly. In other words, the vacancies form

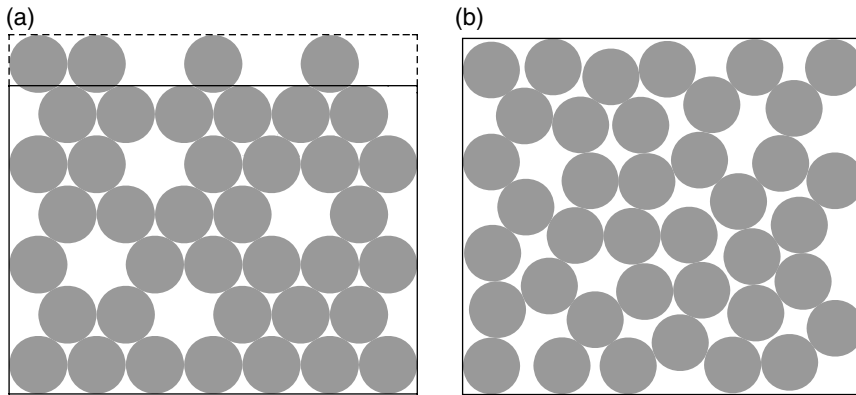


Figure 1.5 Schematic illustration of: (a) vacancies produced in crystal lattice and (b) randomly located holes in a liquid.

empty regions, called *holes*, of various sizes, and atoms/molecules and differently-sized empty spaces are randomly close-packed in the liquid volume (Figure 1.5b). This is the *hole model*. The process of formation of holes is somewhat similar to the formation of vacancies in the crystal lattice and is associated with the thermal motion of atoms/molecules constituting their clusters. However, in contrast to the creation of vacancies by removal of an atom/molecule from far away sites in the interior of the lattice to the crystal surface, ions or clusters are displaced relative to each other by amounts similar to their displacement. Since thermal motion is random and occurs everywhere in the liquid volume, holes are also produced randomly in the liquid. However, holes continuously appear and disappear, move, coalesce to form large holes, and disintegrate into smaller holes.

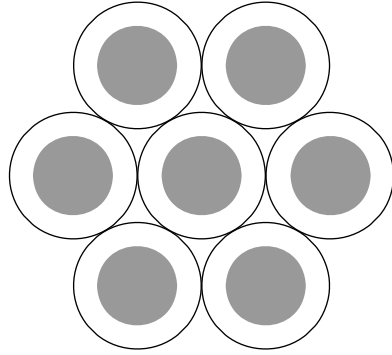
When a gas transforms into the liquid state, the freedom of motion of its atoms/molecules is restricted such that the motion of each of its atoms/molecules is confined within its cell of identical volumes (Figure 1.6). This is the basis of the *simple cell theory*. Every atom/molecule has a free volume available for its motion. If V is the volume of the liquid containing N atoms/particles and v_0 is the volume of each atom/molecule considered as a rigid sphere, the free volume v_f available to each atom/particle for its motion is

$$v_f = \frac{V}{N} - v_0, \quad (1.8)$$

where V/N is the average volume available to each atom/particle.

The restriction in the motion of atoms/molecules to their cells does not explain the transport properties of liquid, entropy of fusion, and volume expansion on melting. These difficulties are overcome in the *liquid free-volume*

Figure 1.6 Free volume available for the motion of its atoms/molecules in a liquid.



theory. According to this theory, the liquid free volume is not distributed equally to each atom/molecule but there is a statistical distribution of free volumes among them and thermal forces are responsible for the statistical distribution of these free volumes.

The movement of an atom/molecule from one position to another not only results in the expansion of the cell of the moving atom/molecule and an increase in its energy but also leads to the contraction of the neighboring cell and a decrease in its energy. This explains the transport properties of liquids. An increase in the volume that occurs on melting implies an increase in the free volume. This means that, except for the free space in the liquid, the atoms/molecules have the same inter-neighbor distance.

The hole model explains most of the experimental observations. Some of the characteristics and predictions of this model are briefly described below.

The formation of holes in the liquid as a result of thermal fluctuations is due to an increase in the vibrations of the liquid molecules around their temporary equilibrium positions. According to the hole theory, the average hole radius r_h is given by (Bockris and Reddy, 1970)

$$r_h = 0.51 \left(\frac{k_B T}{\gamma} \right)^{1/2}, \quad (1.9)$$

where k_B is the Boltzmann constant and γ is the surface tension of the melt. With the values of macroscopic surface tensions γ of different molten salts given in Eq. (1.9), estimates of the values of r_h show that a typical hole is roughly of the size of an ion.

The dependence of self-diffusion coefficient D and viscosity η of simple liquid electrolytes on temperature T follows an Arrhenius-type relation with activation energy E_D for diffusion and activation energy E_η for viscous flow, respectively, related to the melting point T_m by

$$E_D = E_\eta = 3.7R_G T_m. \quad (1.10)$$

Relation (1.9) implies a relationship between the phenomena of diffusion and viscosity in liquids and is associated with the validity of the Stokes–Einstein relation:

$$D = \frac{k_B T}{6\pi r \eta}, \quad (1.11)$$

where r is the radius of moving particles.

Among the different models of liquids, it is found that the hole model is the most consistent model. In the case of ionic liquids, it satisfactorily explains the meaning of activation energy E_η for viscous flow as the work done in transferring a mole of particles from the surroundings of a hole into its interior, experimental compressibilities β and expansion coefficients α_V . It should be mentioned that relation (1.10) holds for nonassociated liquids in which transport processes, such as viscous flow, are determined by the enthalpy of hole formation. However, in associated liquids, such as water, with network structures, the transport process is determined by the energy required to rupture the bonds of the network.

1.3 Water and Other Common Solvents

Different properties of solvents are associated with the structure of particles (i.e. atoms, molecules, or ions) composing them and may broadly be grouped into three categories: (i) static properties, (ii) transport properties, and (iii) thermal properties. Density, refractive index, dielectric constant, and surface tension are essentially static properties and are connected with the statistical distribution of particles composing a liquid. Viscosity and electrical conductivity belong to the transport properties and are associated with the motion of particles in the bulk liquid. In contrast to the viscosity of a liquid that is determined by the relative motion of all particles in the liquid, electrical conductivity is associated with the transport of charged particles. Thermal conductivity, thermal expansivity, and freezing and evaporation of liquids fall in the category of thermal properties and are determined by the thermal motion of particles composing them. In fact, it is the structure of particles that ultimately interact with each other and decide their arrangement and instantaneous distribution in the liquid state and determine the properties of liquids.

Liquid water is commonly employed as a solvent for the crystallization of a wide range of inorganic and organic compounds and its structure and properties are relatively well known. Therefore, it is useful to compare the properties of liquid water with two other simple liquids: methanol and ethanol, which are used for preparing solutions. Some general trends of the behavior of these

solvents are briefly presented here from consideration of the temperature dependence of their density and viscosity under atmospheric conditions.

The temperature dependence of density d of solvents is usually expressed by the polynomial equation:

$$d = d_0 + b_1(T - T_0) + b_2(T - T_0)^2 + b_3(T - T_0)^3 + \cdots + b_n(T - T_0)^n, \quad (1.12)$$

where d_0 is the density of the solvent at temperature T_0 , while b_1 , b_2 , b_3 , and b_n are empirical constants, and T is usually taken in °C. In most cases a quadratic relation usually describes the $d(T)$ data satisfactorily, and the constants b_1 and b_2 are negative quantities. Note that the form of this equation is similar to the equation of the temperature dependence of volume thermal expansivity α_V (see Eq. (1.6)). Another equation relating density d of solvent water with its temperature T is of the form (Szewczyk and Sangwal, 1988):

$$d = d_0 \exp[\beta(T - T_c)^2], \quad (1.13)$$

where d_0 is the solvent density at T_c and β is a constant. Relation (1.13) was originally proposed for aqueous saturated electrolyte solutions (Sangwal, 1987) but has also been reported to hold for aqueous undersaturated solutions (Szewczyk and Sangwal, 1988). Since the density d of a solvent is the inverse of specific volume ϕ_V , it is expected that the dependence of specific volume ϕ_V of solvents, which reflects an expansion of their volume, on solvent temperature T also follows quadratic and exponential equations:

$$\phi_V = \phi_{V0} + \beta_1(T - T_0) + \beta_2(T - T_0)^2, \quad (1.14)$$

$$\phi_V = \phi_{V0} \exp[\beta^*(T - T_c)^2], \quad (1.15)$$

where β_1 , β_2 , and β^* are constants characteristic of the solvent, whereas ϕ_{V0} is the solution specific volume at T_0 in Eq. (1.14) and at T_c in Eq. (1.15).

Figure 1.7a and b shows the dependence of the specific volume ϕ_V and the volume thermal expansivity α_V of water, methanol, and ethanol on their temperature T . The data of Figure 1.7a may be represented by Eq. (1.14), with the parameters listed in Table 1.2, whereas those of Figure 1.7b by Eq. (1.4). Obviously, as seen from the values of the parameters ϕ_{V0} and β_1 , the increase in ϕ_V with temperature is much higher for both alcohols than that for water. Similarly, the thermal expansivity α_V of methanol and ethanol is much higher than that of water. However, in contrast to a nonlinear increase in α_V with temperature for water, the temperature dependence of α_V for methanol and ethanol is linear. These observations of differences in the temperature dependence of specific volume ϕ_V and thermal expansivity α_V of the three solvents are directly associated with the bonds holding their molecules in the liquid state.

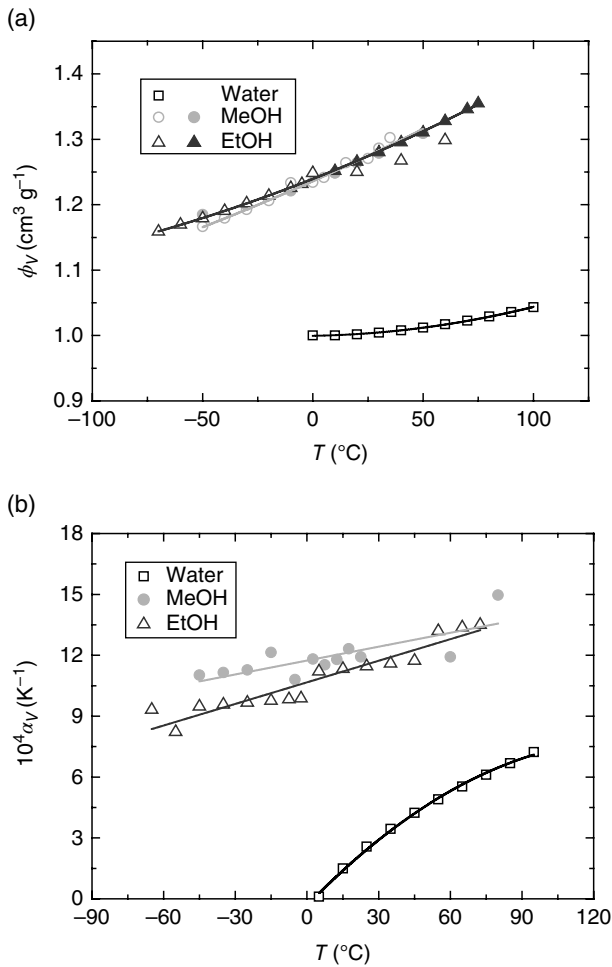


Figure 1.7 Dependence of (a) specific volume ϕ_v and (b) volume thermal expansivity α_v on temperature T of water, methanol, and ethanol. Sources of density data in (a): for water as in Figure 1.1, for methanol from (open circles) www.EngineeringToolBox.com and (filled circles) www.ddbst.com/en, and for ethanol from (open triangles) www.ddbst.com/en and (filled triangles) www.celcius.process.com. Data of (b) calculated from the above data. Data accessed 12 January 2017.

Table 1.2 Values of constants of Eq. (1.14).

Solvent	ϕ_{v0} ($\text{cm}^3 \cdot \text{g}^{-1}$)	$10^3 \beta_1$ ($\text{cm}^3 \cdot \text{g}^{-1} \cdot \text{K}^{-1}$)	$10^6 \beta_2$ ($\text{cm}^3 \cdot \text{g}^{-1} \cdot \text{K}^{-2}$)
Water	0.9996	0.054	3.87
Methanol	1.2362	1.50	1.82
Ethanol	1.2395	1.33	2.58

The temperature dependence of viscosity η of solvents (and melts) may be represented by an Arrhenius-type relation (Bockris and Reddy, 1970; Stokes and Mills, 1965; also see Chapter 9):

$$\eta = \eta_0 \exp\left(\frac{E_\eta}{R_G T}\right), \quad (1.16)$$

where η_0 is the viscosity of the solvent at very high T when the exponential term approaches unity and E_η is the activation energy for viscous flow. Equation (1.16) is derived using the hole theory of liquids (Bockris and Reddy, 1970). Eyring's transition state theory also gives a similar temperature dependence of the viscosity η of solvents, written in the form (Horvath, 1985; Stokes and Mills, 1965):

$$\eta = \frac{h_p N_A}{V^0} \exp\left(\frac{\Delta G^0}{R_G T}\right), \quad (1.17)$$

where V^0 is the molar volume of the solvent, h_p is the Planck constant, and ΔG^0 is the free activation energy for viscous flow of the solvent. Since

$$\Delta G^0 = \Delta H^0 - T \Delta S^0, \quad (1.18)$$

where ΔH^0 and ΔS^0 are the heat and the entropy of activation, respectively, for constant values of ΔS^0 and V^0 , Eq. (1.17) reduces to Eq. (1.16) with $\Delta H^0 = E_\eta$ and $h_p N_A / V^0 \exp(-\Delta S^0 / R_G) = \eta_0$.

The main feature of Eq. (1.17) is that it provides the physical interpretation of the preexponential factor η_0 and the activation energy E_η . According to Eq. (1.16) the dependence of $\ln \eta$ against $1/T$ gives a linear plot with intercept $\ln \eta_0$ and slope E_η / R_G . Figure 1.8 shows plots of $\ln \eta$ against $1/T$ for water, methanol, and ethanol, with the corresponding intercepts $\ln \eta_0$ and slopes E_η / R_G , and the activation energy E_η and the constant $E_\eta / R_G T_m$ calculated therefrom given in Table 1.3.

Two features may be noted from Table 1.3. First, the value of the activation energy E_η for viscous flow is the highest for water, the lowest for methanol, and intermediate between these two values for ethanol. The difference in the values of E_η is due to the processes of creation of holes necessary for their subsequent motion in these solvents and are associated with the nature of chemical bonds in their structures. Second, the ratio $E_\eta / R_G T_m$ is much higher than the expected value of 3.7 of the hole theory of liquids. The high values of $E_\eta / R_G T_m$ are indicators of strong association of the molecules in these liquids. In fact, it is well known that liquid water is an associated liquid.

1.4 Properties of Solutions

A solution is obtained by adding a solute to an appropriate solvent at a given temperature and pressure conditions. A solute may be made up of (i) charged atoms or groups of atoms with negative or positive charges or

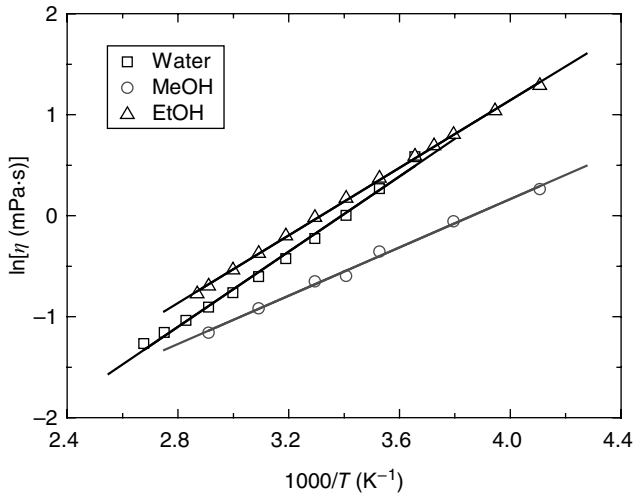


Figure 1.8 Dependence of $\ln\eta$ on $1/T$ for water, methanol, and ethanol. Sources of data: for water from Lide (1996/1997), for methanol from www.EngineeringToolBox.com and www.dbst.com/en, and for ethanol from www.dbst.com/en and www.celcius.process.com. Data for methanol and ethanol accessed 12 January 2017.

Table 1.3 Values of constants of Eq. (1.16).

Solvent	T_m (K)	$-\ln\eta_0$	$10^3 E_\eta/R_G$ (K^{-1})	$10^{-3}\eta_0$ (mPa·s)	E_η ($\text{kJ}\cdot\text{mol}^{-1}$)	E_η/R_G T_m (—)
Water	273.15	6.3108	1.86078	1.817	15.45	6.81
Methanol	175.55	4.6206	1.19616	9.847	9.95	6.81
Ethanol	159.05	5.5499	1.67339	3.888	13.91	10.52

(ii) uncharged neutral molecules. As in the case of liquids, molecular solutes may be composed of polar, nonpolar, or apolar molecules. Although water is the most common solvent and dissolves different types of substances, it is not a universal solvent. It easily dissolves ionic salts but there are many molecular substances that do not dissolve or poorly dissolve in water. The main requirement for the dissolution of a solute in water is that its ions or molecules interact with water molecules to liberate enough energy to break down the water structure. In nonionic solutes, these interactions occur between the O of H_2O molecules and the O and the N of molecular substances, forming hydrogen bonds. For example, in the case of methyl and ethyl alcohols,

hydrogen bonds occur between their O atoms and the O of H₂O. Sugars such as sucrose, C₁₂H₂₂O₁₁, dissolve in water mainly due to hydrogen bonds between their OH groups and O of H₂O molecules. In ionic solutes, however, their dissolution involves lattice breakup, followed by solvation of individual bare ions of splitted lattice.

Ionic solutes dissolved in water or dismantled on melting show conduction of electrical current through the migration of the ions present in the solution. Such ionic solutes and their solutions are known as *electrolytes* and *electrolyte solutions*, respectively. In contrast to these ionic solutes, there is a large number of organic substances dissolved in pure water, which show little conduction. Such solutes are composed of separate, neutral molecules and the bonding of atoms inside the neutral molecules is essentially nonionic. Such solutes and their solutions are known as *nonelectrolytes* and *nonelectrolyte solutions*, respectively.

The above comparative behavior of electrical conduction of solutions is based on water alone used as a solvent. However, when a nonaqueous solvent is chosen to prepare the solution of an electrolyte, the conduction in the solution is reduced tremendously due to the suppressed solvation of its ions by the solvent molecules.

1.4.1 The Solvation Process

In the case of an ionic solute dissolved in small concentrations in solvent water, the solute is dissociated into ions. Thus, the resulting solution consists of solvated ions and solvent water molecules in such a way that the dissociated ions acquire a particular time-averaged spatial distribution in the solution volume. The distance between the solvated ions is large and ion–ion interactions are insignificant in the solution. The process of solvation of ions is a consequence of ion–dipole interactions. Due to these interactions, some of the water molecules are trapped and oriented in the ionic field. The immobile water molecules in the immediate vicinity of the ions during their motion form the *primary solvation sheath*, but in the region between the primary solvation sheath and the bulk water there is also a *secondary region* of loosely-bound water molecules that influence their motion (see Figure 1.9a).

In order to describe the process of solvation of ions in a solvent S, the Born model for ion–solvent interactions may be applied. Following this model, we assume that: (i) one molecule of a solute dissociates into ions considered as rigid spheres of radius r_i and charge $z_i q$, where q is the elementary charge and z_i is the valency of the ion i , (ii) the solvent is a continuum of dielectric constant ϵ_s , and (iii) the interactions between the solvent and the ions are entirely electrostatic. Then the free energy ΔG_{I-S} of ion–solvent interactions per mole of ions is given by (Bockris and Reddy, 1970)

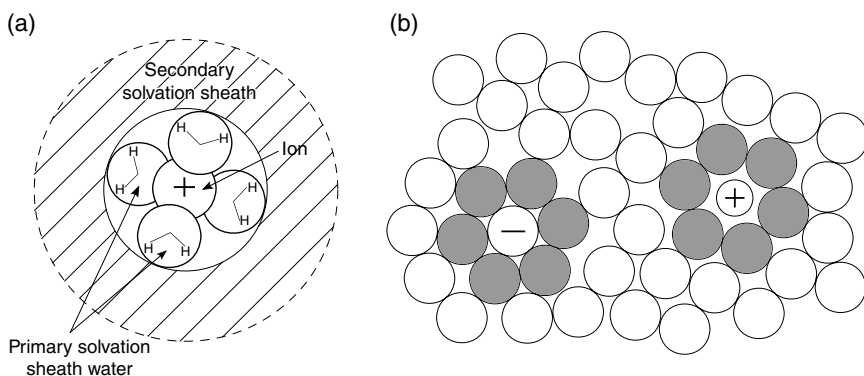


Figure 1.9 (a) Schematic illustration of primary and secondary regions of solvation of a monovalent cation. (b) Free water and immobile hydration water in primary solvation sheaths of ions shown as open and dark circles, respectively. Schematic (a) is based on an illustration in Bockris and Reddy (1970).

$$\Delta G_{I-S} = -N_A k_0 \frac{(z_i q)^2}{2r_i} \left(1 - \frac{1}{\epsilon}\right), \quad (1.19)$$

where the Avogadro number $N_A = 6 \cdot 10^{23}$ ions and the Coulombian proportionality constant $k_0 = 9 \cdot 10^9 \text{ N} \cdot \text{m}^2 \cdot \text{C}^{-2}$. Since $1 \gg 1/\epsilon_s$ (for example, $\epsilon_s = 80$ for water), ΔG_{I-S} is negative, which means that the ions are more stable in the solvent than in a vacuum and the solute is soluble in the solvent of a high dielectric constant. However, when the solvent is replaced by another solvent A of dielectric constant ϵ_a such that $\epsilon_a < \epsilon_s$, the corresponding free energy $|\Delta G_{I-A}| < |\Delta G_{I-S}|$, the ions become relatively less stable and the solute is less soluble in this solvent. Obviously, solute ions more stable in solvent S are more solvated than in solvent A.

When the solute concentration is increased, the average distance between the ions decreases and ion–ion interactions become increasingly important. When the solute concentration is increased further, the water molecules bound to the solvated ions are not effective in dissolving ions further (Figure 1.9b). Then oppositely charged ions come close to form neutrally associated ion pairs. However, since the Coulombian attractive forces $z_+ z_- q^2 / \epsilon_s r^2$ increase with decreasing dielectric constant ϵ_s of the solvent, for nonaqueous solvents of low dielectric constant ion-pair formation is favored. When the Coulombian attractive forces are still strong, ion-pair dipoles may attract ions and form triple ions. Triple-ion formation has been suggested in solvents of $\epsilon_s < 15$, while formation of even still larger clusters of four, five, or even more ions is possible in solvents of $\epsilon_s < 10$.

From the above picture of solvation of ions of an ionic solute immersed in a solvent, it follows that a solution is now composed of randomly distributed solute ions that are surrounded by regions of immobile, strongly trapped solvent molecules around them and randomly distributed molecules of solvents in its remaining volume around the solvated molecules. With increasing solute concentration c , the concentration of solvated ions of the solute increases, whereas the concentration of holes constituting the empty space in the solvent decreases. Therefore, the dependence of the properties of solutions of a solute on solute concentration c dissolved in a solvent is determined by the processes of solvation of solute ions and creation of holes.

Here, it should be remembered that the solvated ionic entities participating in the properties of solutions are larger than the bare, unsolvated ions because of the firmly trapped water molecules around them. Therefore, the radius of the kinetic entity participating in the transport properties of solutions is expected to change from one solvent to the other because of changes in the structure of the solvation sheath. Since solvent molecules constitute the firmly-trapped solvation sheath, the sizes of these firmly-trapped solvent molecules mainly contribute to the changes in the radii of the solvated ions. For example, in the case of solvents water, methanol, and ethanol, the size of the molecules increases in the order: water, methanol, and ethanol; the radius of the solvated ions also increases in this order.

Finally, it should be emphasized that in the solvation of a solute, normal extensive hydrogen-bonded structure of water, in general, responds to the presence of solute molecules and ions by spatial and orientational arrangements, which result in an overall increase in the order of the solution. Interactions of ions with the dipole of water molecules lead to their solvation but hydrophobic interactions are the predominant factor in the solvation of nonpolar or apolar molecules. In an aqueous solution of polar solutes, their molecules break down the hydrogen-bonded arrangement of water and replace it with a spherically symmetrical non-hydrogen-bonded shell of water molecules. In a nonelectrolyte, there is no dissociation of its molecules and the solute molecules retain their unbroken identity.

1.4.2 The Concentration of Solutions

Concentration of a solute dissolved in a solvent is expressed in different ways. Among the commonly used ways are: (i) mass composition or weight fraction concentration, usually given in percentage, relative to the solvent, which is the ratio of the mass of the solute dissolved to the mass of the solvent, (ii) weight fraction concentration, also given in percentage, relative to the solution, which is the ratio of the mass of the solute dissolved to the mass of the solution, (iii) molar concentration c , which is the ratio of the number of moles of the solute to the volume of the solution taken in moles per liter, i.e. $\text{mol}\cdot\text{dm}^{-3}$ denoted

by the symbol M , (iv) molal concentration m , which is the ratio of the number of moles of the solute contained in 1 kg of the solvent, and (v) mole fraction x , which is the ratio of the number of moles of the dissolved solute to the sum of the number of the moles of all components of the solution (symbol m). For preparing saturated solutions both individual solvents as well as mixtures of solvents are used. Molar and molal concentrations are frequently used to express solute concentration in aqueous solutions but weight percent concentration relative to the solvent are usually used to express concentration in different individual solvents and their mixtures. However, temperature dependence of solubility of various solutes in solutions is customarily expressed in mole fraction x , defined as

$$\begin{aligned} x \text{ (mole fraction)} &= \frac{\text{moles of solute in solution}}{\text{sum of moles of solute and solvent in solution}} \\ &= \frac{W_S/M_S}{W_S/M_S + W_F/M_F}, \end{aligned} \quad (1.20)$$

where W_S and W_F are the masses and M_S and M_F are the molecular masses of solute S and solvent F (F for fluid), respectively. The commonly used units for solute concentration are given below:

$$M \text{ (molarity)} = \frac{\text{moles of solute}}{1000 \text{ ml solution}} = \frac{W_S/M_S}{1000 \text{ ml solution}}, \quad (1.21)$$

$$m \text{ (molality)} = \frac{\text{moles of solute}}{1000 \text{ g solvent}} = \frac{W_S/M_S}{1000 \text{ g solvent}}. \quad (1.22)$$

Apart from the above units, some other frequently used units are as follows:

$$c_W \text{ (wt. fraction)} = \frac{\text{mass of solute}}{\text{mass of solvent}} = \frac{W_S}{W_F}, \quad (1.23)$$

$$c_W^S \text{ (wt. fraction)} = \frac{\text{mass of solute}}{\text{mass of solution}} = \frac{W_S}{W_F^S} = \frac{W_S}{W_F + W_S} = c_W(1 + c_W)^{-1} < c_W, \quad (1.24)$$

$$c_m \text{ (molar ratio)} = \frac{\text{moles of solute in solution}}{\text{moles of solvent in solution}} = c_W \frac{M_F}{M_S}. \quad (1.25)$$

In Eq. (1.24), W_F^S is the mass of the solution. In the case of a mixture of two miscible solvents 1 and 2, concentration x^* in mole fraction may be given by

$$x^* \text{ (mole fraction)} = \frac{W_S/M_S}{W_S/M_S + (W_1/M_1)\{(1-X) + X(M_1 W_2/M_2 W_1)\}}, \quad (1.26)$$

where the composition of the solvent mixture is expressed in moles and X is the molar content of solvent 2. When $X = 0$ or $W_1/M_1 = W_2/M_2$, the above expression reduces to Eq. (1.21).

1.4.3 Density and Thermal Expansivity of Solutions

Dependence of density d of solutions on solute concentration c , expressed in moles, in their solutions in a solvent at a given temperature T is usually described by the relations:

$$d = d_0 + k_1c + k_2c^2, \quad (1.27)$$

$$d = d_0 + \frac{c}{k_3 + k_4c}, \quad (1.28)$$

where k_1 , k_2 , k_3 , and k_4 are empirical constants, and d_0 is the density of the solvent when $c = 0$. Usually, the change in solvent density d_0 with the addition of a solute is less than 10%. Therefore, Eq. (1.28) takes the form of Eq. (1.27), with $k_1 = 1/k_3$ and $k_2 = -k_4/k_3^2$. Using Eq. (1.27) one can also write the solute concentration dependence of solution specific volume in the form:

$$\phi_V = \phi_{V0} - k_5c + k_6c^2, \quad (1.29)$$

where $k_5 = \phi_{V0}/k_3 = k_1\phi_{V0}$ and $k_6 = \phi_{V0}k_4/k_3^2 = -k_2\phi_{V0}$.

When the constant $k_2 = 0$ in Eq. (1.27), the solution density d increases and its specific volume ϕ_V , given by Eq. (1.29), decreases linearly with an increase in solute concentration c . The linear dependence of density d of a solution may be obtained from the additivity rule in the form:

$$d = d_0(1-x) + d^*x = d_0 + (d^* - d_0)x = d_0 + 10^3c(M^* - KM_s), \quad (1.30)$$

where x and $(1-x)$ are the mole fractions of the solute and the solvent in a solution, respectively, d_0 and d^* are their corresponding densities, M_s and M^* are their molar masses, respectively, and K is the packing coefficient of the solute. Application of the additivity rule to specific volumes ϕ_{V0} and ϕ_V^* of solvent and solute, respectively, also gives a similar relation, i.e.

$$\phi_V = \phi_{V0}(1-x) + \phi_V^*x = \phi_V^* - (\phi_{V0} - \phi_V^*)x = \phi_{V0} - 10^3c(KM_s - M^*). \quad (1.31)$$

The packing coefficient K of the solute is defined as the ratio of apparent molar volume Φ of the solute to the molar volume V^0 of the solution, i.e. $K = \Phi/V^0$. The value of the packing coefficient K of a solute is practically a constant quantity and depends only on the solution temperature T . Its value is determined by the solvation process.

As in the case of the dependence of the density d and the specific volume ϕ_V of the solution of a solute in a given solvent at a given temperature T on the solute concentration c , the concentration dependence of the solution expansivity α_V at the given temperature also follows the quadratic equation:

$$\alpha_V = \alpha_{V0} + \alpha_3 c + \alpha_4 c^2, \quad (1.32)$$

where α_{V0} is the expansivity of the solvent at the temperature T and α_3 and α_4 are constants characterizing the solute concentration in the solution.

Figure 1.10 shows, as examples, the dependences of specific volume ϕ_V and volume thermal expansivity α_V on NaCl concentration in aqueous solutions at two selected temperatures of 25 and 80 °C. The dependences of ϕ_V and α_V on the solute concentration may be described by Eqs. (1.29) and (1.32), respectively, with the values of the constants given in Table 1.4.

It may be noted from the $\phi_V(c)$ plots that the constants k_5 and k_6 are practically temperature independent. As seen from Eq. (1.31), this is a result of the temperature independence of the packing coefficient K . From the $\alpha_V(c)$ plots, on the other hand, one observes changes in the signs of the constants α_3 and α_4 , the transition taking place at a temperature of about 60 °C. This type of behavior is also observed for other electrolytes dissolved in water (see Horvath, 1985) and is associated with the adiabatic compressibility β_S of electrolyte solutions (see below), which go through minima between 50 and 70 °C for alkali metal chlorides.

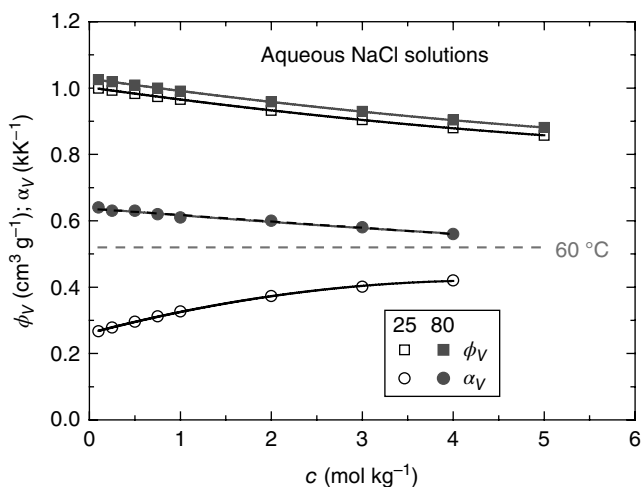
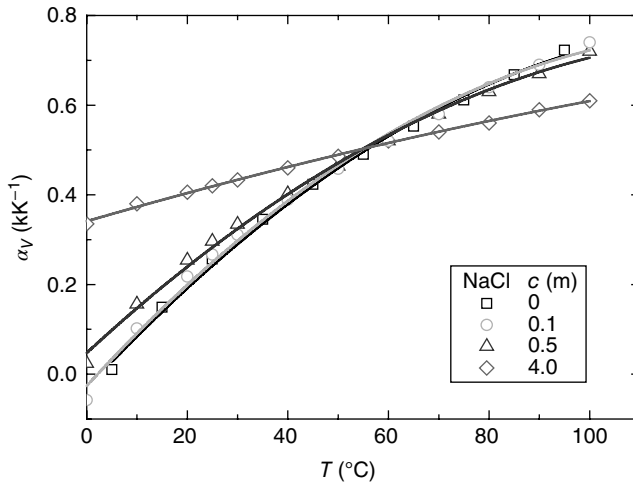


Figure 1.10 Dependence of specific volume ϕ_V and volume thermal expansivity α_V on NaCl concentration in aqueous solutions at 25 and 80 °C. Temperatures given in the inset is in °C. Dashed line shows a transition in $\alpha_V(c)$ dependence taking place at a temperature of about 60 °C. Source: Original data from Lide (1996/1997).

Table 1.4 Constants of Eqs. (1.29) and (1.32) for aqueous NaCl solutions.

T (°C)	Eq. (1.29)			Eq. (1.32)		
	ϕ_{V0} ($\text{cm}^3 \cdot \text{g}^{-1}$)	$-10^{-2}k_5$ (l mol^{-1})	$10^{-3}k_6$ ($\text{kg} \cdot \text{l} \cdot \text{mol}^{-2}$)	$10^{-3}\alpha_{V0}$ (K^{-1})	$10^{-5}\alpha_3$ ($\text{kg} \cdot \text{mol}^{-1} \cdot \text{K}$)	$10^{-6}\alpha_3$ ($\text{kg}^2 \cdot \text{mol}^{-2} \cdot \text{K}$)
25	1.0021	3.866	1.92	0.261	7.22	-8.21
80	1.0282	3.866	1.85	0.628	-2.25	0.83

**Figure 1.11** Dependence of volume thermal expansivity α_V on solution temperature T for three selected NaCl concentrations c in aqueous solutions. NaCl concentration c given in the inset is in molality. Original data from Lide (1996/1997). *Source:* Data for water from Figure 1.3.

The dependence of volume thermal expansivity α_V of solutions on their temperature T follows the same relation as relation (1.6) observed for solids and liquids. Figure 1.11 shows the experimental data of the volume thermal expansivity α_V of aqueous NaCl solutions of three selected concentrations c as a function of their temperature T , where the plots are drawn with the best-fit constants listed in Table 1.5. The data for water are from Figure 1.3. From the plots the following features may be noted:

- 1) The initial value of the expansivity α_{V0} at 0 °C increases with increasing concentration c .
- 2) The increase in the expansivity α_V with temperature is retarded by the addition of the solute to the solvent water.

Table 1.5 Constants of Eq. (1.6) for aqueous NaCl solutions.

c (m)	$10^{-5}\alpha_{V0}$ (K ⁻¹)	$10^{-5}\alpha_1$ (K ⁻²)	$10^{-8}\alpha_2$ (K ⁻³)
0	-3.13 ± 1.23	1.207 ± 0.057	-4.49 ± 0.55
0.1	-2.62 ± 1.27	1.220 ± 0.064	-4.72 ± 0.62
0.5	4.76 ± 1.07	1.036 ± 0.047	-3.77 ± 0.45
4.0	34.11 ± 0.31	0.327 ± 0.015	-0.57 ± 0.14

- 3) All plots intersect at a temperature of about 55 °C, suggesting a limiting value of temperature-independent α_V of about 0.48 kK⁻¹.

These features may be understood from the observed relationship between α_V of the solutions and isothermal and adiabatic compressibilities β_T and β_S , given by (see Horvath, 1985)

$$\alpha_V^2 = \left(\frac{\beta_T - \beta_S}{T} \right) C_p, \quad (1.33)$$

where C_p is the heat capacity at constant pressure per unit volume.

Figure 1.12a shows typical examples of the dependence of density d of aqueous ammonium oxalate (chemical formula: $(\text{NH}_4)_2\text{C}_2\text{O}_4$; abbreviation: Am2Ox) and sodium oxalate (chemical formula: $\text{Na}_2\text{C}_2\text{O}_4$; abbreviation: Na2Ox) solutions of selected concentrations on solution temperature T . The plots of the $d(T)$ data are drawn according to Eq. (1.12) with the best-fit parameters listed in Table 1.6. Figure 1.12b shows the specific volumes ϕ_V calculated from the above $d(T)$ data as a function of $(T - T_c)^2$ according to Eq. (1.15), whereas the plots are shown with the parameters included in Table 1.6. In the figure, concentration is given in mol·l⁻¹.

From Figure 1.12a it may be noted that in the case of ammonium oxalate solutions, the value of d_0 increases, whereas the values of both b_1 and b_2 decrease with an increase in solution concentration c . The values of d_0 , b_1 , and b_2 of Eq. (1.12) for 0.2 mol·l⁻¹ sodium oxalate solution are different from those for 0.2 mol·l⁻¹ ammonium oxalate solution. However, from Figure 1.12b it may be noted that in the range of concentration of ammonium oxalate solutions studied here, the value of ϕ_{V0} decreases with increasing solution concentration c , whereas those of β^* and T_c are independent of concentration c . The values of ϕ_{V0} , β^* , and T_c for 0.2 mol·l⁻¹ sodium oxalate solution are different from those for 0.2 mol·l⁻¹ ammonium oxalate solution. These trends are associated with the solvation characteristics of the cations and anions of the salts and the effect of temperature on the solvation process. In comparison with ammonium oxalate, more changes are caused by sodium oxalate because of its smaller size, which results in more hydrated Na⁺ ions than NH₄⁺ ions.

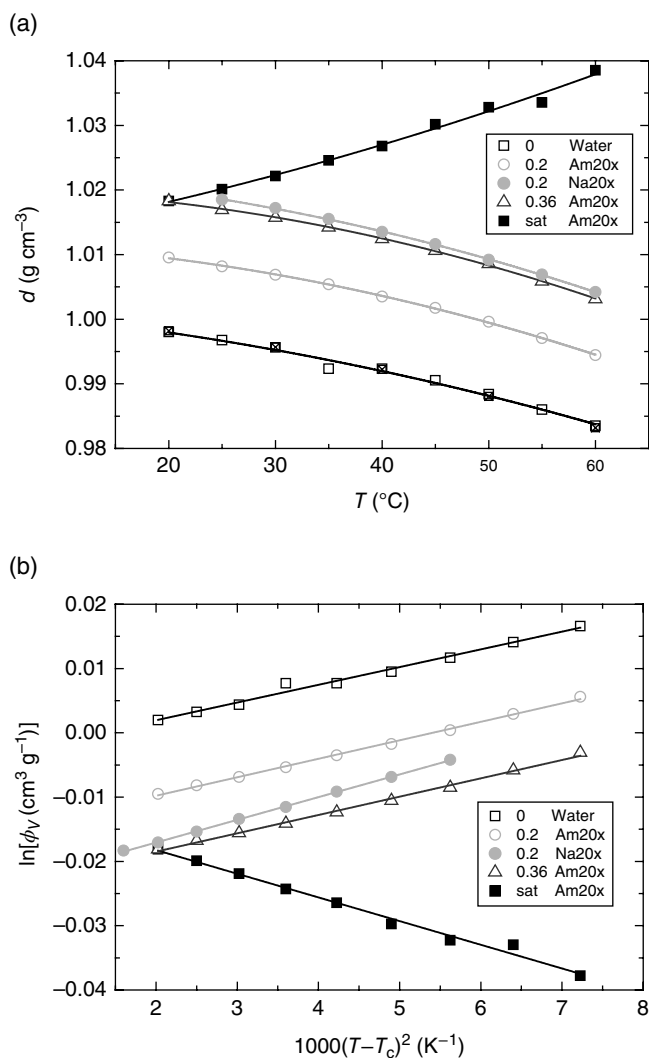


Figure 1.12 Dependence of (a) density d of aqueous ammonium oxalate (Am2Ox) and sodium oxalate (Na2Ox) solutions of selected concentrations on solution temperature T , with best-fit plots drawn according to Eq. (1.12) and (b) specific volume ϕ_v calculated from the above $d(T)$ data on $(T - T_c)^2$ according to Eq. (1.15). Concentration shown in the insets is given in mol·l⁻¹. For comparison, density d and specific volume ϕ_v of saturated Am2Ox solutions at different temperatures are also presented. *Source:* Original data of Am2Ox and Na2Ox from Frej et al. (2000) and Misztal (2004), respectively.

Table 1.6 Constants of Eqs. (1.12) and (1.15) for aqueous Am2Ox and Na2Ox solutions.

c (mol·l ⁻¹)	Salt	Eq. (1.12)				Eq. (1.15)			
		d_0 (g·cm ⁻³)	$-10^{-4}b_1$ (g·cm ⁻³ ·K)	$-10^{-6}b_2$ (g·cm ⁻³ ·K ²)	$-10^{-2} \ln \phi_{v0}$	$10^{-6}\beta^*$ (K ⁻²)	T_c (K)	$10^{-11}\beta^*/T_c^2$ (-)	
0		1.0017	1.2906	2.82	0.036	2.76	298	3.11	
0.2	Am2Ox	1.0120	0.4585	4.09	1.554	2.87	298	3.23	
0.2	Na2Ox	1.0229	0.7452	-39.5	2.413	3.53	288	4.25	
0.36	Am2Ox	1.0201	0.0493	4.60	2.419	2.85	298	3.21	
sat.	Am2Ox	1.0114	-2.8645	-2.59	1.087	-3.68	298	-4.14	

Finally, it may be concluded that the above trends of $d(T)$ or $\phi_V(T)$ data of electrolyte solutions of particular concentrations are connected with the volume thermal expansivity α_V . However, although both equations describe the $d(T)$ and $\phi_V(T)$ data for solutions of different concentrations, Eq. (1.15) characterizes them for an electrolyte in terms of two constants d_0 (or $\phi_{V0} = 1/d_0$) and the dimensionless concentration-independent parameter β^*/T_c^2 . Higher values of d_0 and β^*/T_c^2 represent more solvated ions.

1.4.4 Viscosity of Solutions

Figure 1.13 shows, as an example, the dependence of viscosity η of aqueous sucrose solutions at three selected temperatures on its concentration c . As is the general trend of the dependence of the viscosity η of solutions of different compounds, for the solution of a given concentration the viscosity η decreases with increasing temperature T , but at a given temperature the viscosity η of a solution initially increases practically linearly with concentration c up to about 35% and then increases rapidly. Obviously, in addition to solvent molecules, solvated entities participate in the viscous flow of solutions and both the composition of a solution in a solvent and the temperature of the solution determine its viscosity.

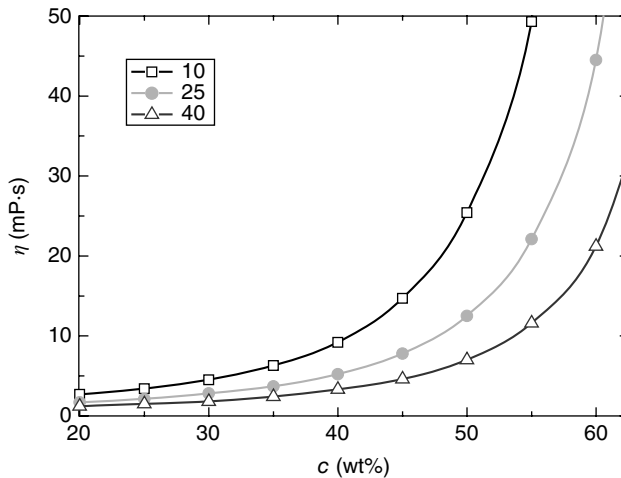


Figure 1.13 Dependence of viscosity η of aqueous sucrose solutions at three selected temperatures ($^{\circ}\text{C}$) on its concentration c . Temperature in the inset is in $^{\circ}\text{C}$. Original data from Asadi (2006).

To account for the effect of solute concentration in a solution, Jones and Dole gave the empirical relation (Horvath, 1985; Stokes and Mills, 1965):

$$\frac{\eta}{\eta^0} = 1 + Ac^{1/2} + Bc, \quad (1.34)$$

where η_0 is the viscosity of the solvent, and A and B are constants, which depend on solution temperature and are characteristic for an electrolyte. The ratio η/η_0 is the relative solution viscosity. However, this equation describes the viscosity data for relatively dilute electrolyte solutions. To describe concentrated solutions, a modified form of the above relation has been used (Horvath, 1985; Stokes and Mills, 1965), i.e.

$$\frac{\eta}{\eta^0} = 1 + Ac^{1/2} + Bc + Cc^2, \quad (1.35)$$

where C is an empirical constant.

The second term, with the constant A , on the right of Eq. (1.35) accounts for long-range Coulomb forces between the ions considered as point charges. The constant A is expected to be a positive quantity. However, this contribution from ion–ion interaction to the viscosity of electrolyte solutions is very small and explains the experimental $\eta(c)$ data only in very dilute solutions. At concentrations above about 0.002 M, a linear increase in viscosity with solute concentration is observed in strong electrolytes extending to 0.1 M and higher in aqueous solutions and to somewhat lower concentrations in some nonaqueous systems. In this concentration range, the B coefficient can be positive as well as negative, depending on the solute, the solvent, and the solution temperature. The origin of this B coefficient lies in ion–solvent interactions. Negative B coefficients are found for electrolytes composed of large ions in associated solvents such as water at relatively low temperatures. For example, at 25 °C, KCl and KI in aqueous solutions have negative B coefficients but NaCl in aqueous solutions has a positive B coefficient. However, KCl and KBr in methanol solutions have positive B coefficients.

The values of A and B parameters of Eq. (1.34) may be separated by plotting $[(\eta/\eta^0) - 1]/c^{1/2}$ against $c^{1/2}$ of the $\eta(c)$ data for a compound. The linear plot gives the intercept A and the slope B . Figure 1.14 shows, as an example, the dependence of $[(\eta/\eta^0) - 1]/c^{1/2}$ on $c^{1/2}$ of aqueous sodium oxalate (Na_2Ox) solutions at three selected temperatures according to Eq. (1.34). The plots, drawn with the constants listed in Table 1.7, show that the value of parameter A decreases and that of B increases with an increase in solution temperature T . Some comments on these observations deserve attention.

The A parameter is a measure of ion–ion interaction involved in a salt dissolved in a given solvent and the temperature (Horvath, 1985; Stokes and Mills, 1965). Its value essentially depends on the valency of ions composing the salt and is a positive quantity. In contrast to the expected positive values of A , its

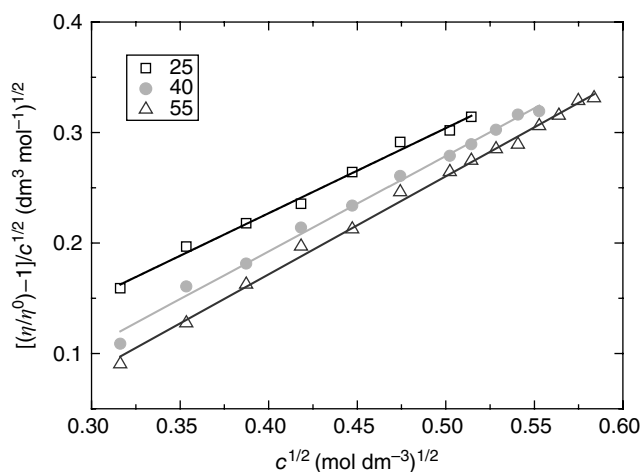
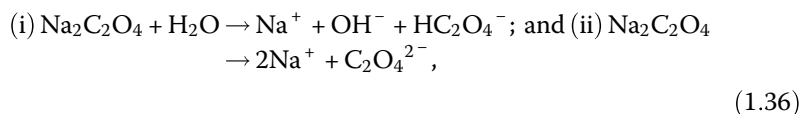


Figure 1.14 Dependence of viscosity $[(\eta/\eta^0) - 1]/c^{1/2}$ on $c^{1/2}$ of aqueous sodium oxalate (Na_2Ox) solutions at three selected temperatures according to Eq. (1.34). Temperature in the inset is in $^\circ\text{C}$. Original data from Misztal (2004).

observed negative values may be due to a large scatter in the values of η/η^0 at different concentrations and temperatures. This discrepancy may also be due to the interaction of relatively large anions (i.e. HC_2O_4^- or $\text{C}_2\text{O}_4^{2-}$ ions) and solvent molecules. The decrease in the value of A of the solutions with increasing temperature may be associated with weakening of ion–ion interactions in the solution, which leads to a diminution in the process of association of ions and solute molecules. In other words, when solvated ions form associates at low temperatures, the tendency of formation of molecular associates decreases with increasing temperature of the solution due to the decreasing ability of formation of bonds between the existing ions and the solvent molecules.

The value of the B parameter for electrolyte solutions is a sum of the values of contributions of cations and anions and depends on temperature (Horvath, 1985; Stokes and Mills, 1965). Assuming that dissolution of $\text{Na}_2\text{C}_2\text{O}_4$ in water results in the following ions:



where all ions are solvated, with the contributions of about 0.09 and 0.10 $\text{mol}\cdot\text{dm}^{-3}$ for Na^+ and OH^- ions, respectively, at 30°C (Horvath, 1985), one finds the contribution of HC_2O_4^- and $\text{C}_2\text{O}_4^{2-}$ ions to the B parameter, denoted by B_{2-} in Table 1.7, is practically the same and lies between 0.6 and

Table 1.7 Constants of Eq. (1.34) at different temperatures for aqueous Na₂O_x solutions.

T (°C)	A (dm ^{3/2} ·mol ^{-1/2})	B (dm ³ ·mol ⁻¹)	B_{2-} (dm ³ ·mol ⁻¹)
25	-0.081 ± 0.011	0.770 ± 0.026	0.59
40	-0.153 ± 0.010	0.863 ± 0.022	0.68
55	-0.183 ± 0.008	0.887 ± 0.016	0.70

0.7 mol·dm⁻³, which gives the average anionic volume $V_a = 2.56 \cdot 10^{-27}$ m³ and the radius $r_a = 0.85$ nm.

The B coefficients for various salts in aqueous and methanolic solutions are related to the molar entropy ΔS^0 of solution corrected for the so-called cratic contribution S^* of the solvent entropy, i.e. corrected solution molar entropy = $\Delta S^0 - S^*$. The solution molar entropy ΔS^0 is defined as the difference between the molar entropy S_c of the crystal and the partial molar entropy S_s in a hypothetical ideal 1 M solution, i.e. $\Delta S^0 = S_s - S_c$.

Depending on the strength or weakness of the bond between the ion and the solvent molecules in the primary solvation sheath, water molecules are strongly bound to the surface of some of the ions than the water molecules among themselves (structure-making ions), whereas they are weakly bound to the surface of other ions (structure-breaking ions). Because of higher charge density, ions having small size and high valency such as Li⁺, Mg²⁺ and La³⁺, bind the water molecules strongly and are structure makers while ions having relatively large size and low valency behave as structure breakers. The B coefficient of a solute-solvent system is usually considered as the sum of contributions made by the solute cations and anions, and these B_i coefficients of ions have been related to their other properties. For example, the ionic B_i coefficients for both monoatomic and polyatomic ions decrease with increasing partial molar entropies of hydration at 25 °C, and the ionic B_i coefficients increase with increasing hydrated ionic volumes V_H .

The viscosity of a liquid is the result of relative motion of its particles. Therefore, it is expected that electrolyte solutions containing large ions relative to the solvent molecules will have a viscosity higher than that of the solvent. Assuming that the ions behave as rigid spheres suspended in a continuum, the viscosity η of the suspension in a medium of viscosity η^0 may be given by the Einstein relation

$$\frac{\eta}{\eta^0} = 1 + 2.5\phi, \quad (1.37)$$

where ϕ is the volume fraction of the particle in the medium. This relation holds for solution of small ϕ . To deal with higher concentrations of particles, Vand proposed the relation

$$\ln\left(\frac{\eta}{\eta_0}\right) = \frac{2.5\phi}{1-Q\phi}, \quad (1.38)$$

where Q is a parameter characterizing the mutual interaction between the liquid surface layers. For small volume fractions ϕ , this equation reduces to Eq. (1.37).

For small values of ϕ , $\phi = cV_m$, where c is the solute concentration in $\text{mol}\cdot\text{l}^{-1}$ and V_m is the molar volume in $\text{l}\cdot\text{mol}^{-1}$. Then Eq. (1.38) takes the form

$$\ln\left(\frac{\eta}{\eta^0}\right) = \frac{B_2c}{1-Q'c}, \quad (1.39)$$

where $B_2 = 2.5V_m$ and $Q' = QV_m$. When $Q'c \ll 1$, Eq. (1.39) reduces to the form of Eq. (1.34), with $Ac^{1/2} \ll Bc$ and $B = 2.5V$.

Eyring's transition-state theory has extensively been used to explain the dependence of solution viscosity η on solute concentration c and solution temperature T (for example, see: Feakins et al., 1974, 1993; Goldsack and Franchetto, 1977, 1978; Horvath, 1985). A simplified version of this approach is presented below.

Using Eyring's transition-state theory, the solution viscosity η may be given by (Goldsack and Franchetto, 1977, 1978)

$$\eta = \frac{h_p N_A}{V} \exp\left(\frac{\Delta G}{R_G T}\right), \quad (1.40)$$

where V and ΔG are the molar volume and the free energies of activation for the solution, respectively. When the values of V and ΔG of the solution are the sums of contributions of solvent and solute, defined by

$$V = (1-x)V^0 + xV^S = V^0[1 + x(V^S - V^0)/V^0], \quad (1.41)$$

and

$$\Delta G = (1-x)\Delta G^0 + x\Delta G^S = \Delta G^0[1 + x(\Delta G^S - \Delta G^0)/\Delta G^0]. \quad (1.42)$$

Eq. (1.40) gives

$$\eta = \frac{h_p N_A}{V^0(1+xV)} \exp\left(\frac{\Delta G^0(1+xF)}{R_G T}\right), \quad (1.43)$$

and

$$\frac{\eta}{\eta^0} = \frac{1}{1+xV} \exp\left(\frac{xF}{R_G T}\right), \quad (1.44)$$

where x is the solute concentration expressed in mole fraction, the solvent viscosity η^0 is given by Eq. (1.17), F is the activation energy required for the formation of a hole in the solution, and V and F are constants for different types of salts and depend on the solution temperature. Equation (1.43) takes the form of Eq. (1.17) when

$$\frac{1}{\eta_0} = \frac{V^0}{h_p N_A} (1 + xV) \quad (1.45)$$

$$E_\eta = \Delta G^0 (1 + xF). \quad (1.46)$$

For an $n : 1$ salt the constants V and F are given by

$$V = \frac{V^S - V^0}{V^0} = \frac{nV_c + V_a}{V^0} - (n + 1), \quad (1.47)$$

$$F = \frac{\Delta G^S - \Delta G^0}{\Delta G^0} = n\Delta G_c + \Delta G_a - (n + 1)\Delta G^0. \quad (1.48)$$

In the above equations the superscripts S and 0 with the molar volume V and the free energy ΔG denote solute and solvent, respectively.

According to Eq. (1.43), addition of a solute to the solvent leads to a change in the viscosity η by changes in both the preexponential factor η_0 and the activation energy ΔG^0 , and the B coefficient is related to the constants V and F . For aqueous electrolyte solutions the approximate relation is (Horvath, 1985)

$$B = \frac{(F/R_G T) - V}{55.51}, \quad (1.49)$$

with V and F given by Eqs. (1.47) and (1.48), respectively.

The above approach of the temperature dependence of the viscosity of solutions is useful in understanding the effect of solute concentration and obtaining the size of entities involved in viscous flow and crystallization of the solute. As an illustration, the experimental data of the temperature dependence of viscosity of aqueous ammonium oxalate solutions of different concentrations, reported by Frej et al. (2000), are considered. Figure 1.15 shows examples of the dependence of $\ln \eta$ of aqueous ammonium oxalate solutions of four selected concentrations and solvent water on $1/T$ according to Eq. (1.43). In the figure the plot for water represents the temperature interval between 15 and 50 °C. As seen from the figure, the plots of $\ln \eta$ against $1/T$ follow linear dependence with intercept $\ln \eta_0$ and slope E_η/R_G for different solute concentrations x (expressed in mole fraction) such that the linear plots of $\ln \eta$ against $1/T$ for the solutions are shifted upward relative to the plot for water and the shift increases with the solute concentration x in the solution. The various values of the intercept $\ln \eta_0$ and the slope E_η/R_G for different aqueous ammonium oxalate solutions obtained by Sangwal et al. (2004) are plotted as a function of concentration x according to Eqs. (1.45) and (1.46) in Figure 1.16. In Figure 1.16, two values of the intercept and the slope corresponding to $\eta(T)$ data for water in the temperature intervals between 15 and 50 °C and between 15 and 55 °C are presented to show that the extrapolated values of E_η/R_G and $\ln \eta_0$ for $x = 0$ can differ substantially from the values obtained from the experimental $\eta(T)$ data for water, depending on the temperature interval of the data considered as a

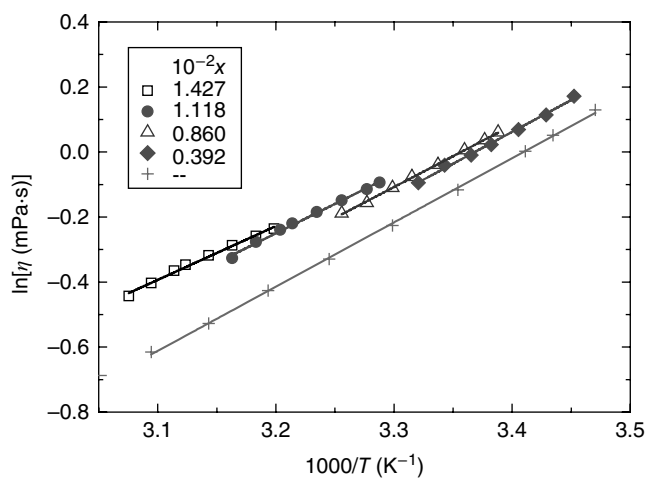


Figure 1.15 Dependence of $\ln\eta$ of aqueous ammonium oxalate (Am_2Ox) solutions of four selected concentrations and water on $1/T$ according to Eq. (1.43). Solute concentration x shown in the inset is given in mole fraction. *Source:* Original data for ammonium oxalate solutions and water are from Frej et al. (2000) and Lide (1996/1997), respectively.

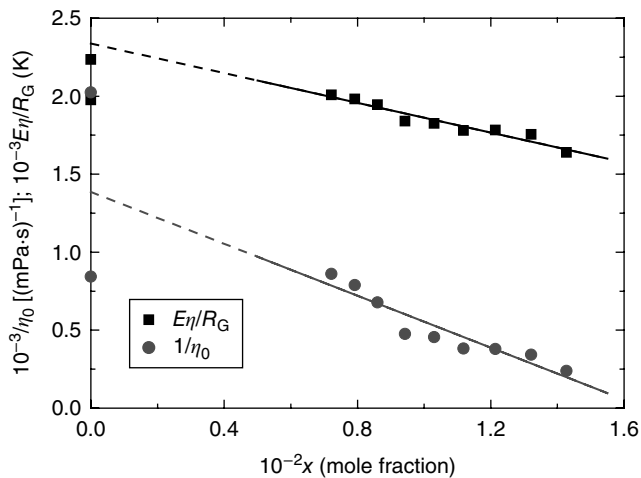


Figure 1.16 Relationship between $1/\eta_0$ and E_η/R_G on the concentration c of aqueous ammonium oxalate (Am_2Ox) solutions according to Eq. (1.52). *Source:* Data from Sangwal et al. (2004).

Table 1.8 Estimated values of different constants from Eqs. (1.45) and (1.46).

Equation	Intercept	Slope			
(1.45)	$V^0/h_p N_A = 1386 \pm 120$ (mPa·s) ⁻¹	$10^{-4}V^0 = 5.5 \pm 0.5$ m ³ ·mol ⁻¹	$r^0 = 0.60 \pm 0.02$ nm	$-10^{-3}V^a = 1.09 \pm 0.15$ m ³ ·mol ⁻¹	$r = 0.76 \pm 0.03$ nm
(1.46)	$10^3\Delta G^0/R_G = 2.338 \pm 0.051$ K	$\Delta G^0 = 19.4 \pm 0.5$ kJ·mol ⁻¹		$-10^4F/R_G = 4.76 \pm 0.47$ K	$F = 396 \pm 39$ kJ·mol ⁻¹

Source: After Sangwal et al. (2004).

^a From plot original $V = -60 \pm 8$ (mole fraction)⁻¹.

reference. From the values of the intercept and the slope of the linear plots of Figure 1.16, the values of different quantities are given in Table 1.8.

It may be noted from Table 1.8 that both V and F are negative. This means that in the case of aqueous ammonium oxalate solution the following relations hold (cf. Eqs. (1.47) and (1.48)):

$$2V_c + V_a < 3V_0, \quad (1.50)$$

$$(2\Delta G_c + \Delta G_a) < 3\Delta G^0. \quad (1.51)$$

These relations indicate that the values of the activation energies are essentially determined by the size of ions and solvent molecules. The crystallographic radii of H₂O molecules, and NH₄⁺ and HC₂O₄⁻ ions are 0.138 nm, 0.148 nm, and about 0.20 nm. Therefore, it may be inferred that the average radius r_{H_2O} of holes due to water molecules in the solvent responsible for the viscous flow of water is greater than 0.168 nm.

Extrapolation of the plot of E_η/R_G against x to $x = 0$ gives the value of $\Delta G^0 = 19.4 \pm 0.5$ kJ·mol⁻¹ (see Table 1.8). This value of ΔG^0 agrees well with the value of 18.6 kJ·mol⁻¹ for viscous flow of water at high temperatures. Since both E_η and η_0 of solutions depend on solute concentration x , they are also mutually related (see Figure 1.20) and follow the expression (Sangwal et al., 2004):

$$\frac{E_\eta}{R_G} = A_1 - B_1 \ln \eta_0, \quad (1.52)$$

with constants: $A_1 = 97.5 \pm 23.7$ K and $B_1 = 282.9 \pm 3.8$ K. Rewriting this equation in the form of Eq. (1.17), one finds a new temperature $T^* = B_1 = 282.9 \pm 3.8$ K and a new preexponential factor $A_1/B_1 = \ln \eta_0^* = 0.344 \pm 0.08$ or $\eta_0^* = 1.406$ mPa·s, which gives the corresponding volume $V^* = h_p N_A / \eta_0^* = 4.71 \cdot 10^{-31}$ m³. From the value of the solvent hole volume V^0 (see Table 1.8) and the above volume V^* , one obtains the solvent hole radius $r^0 = 0.604$ nm and the critical radius $r^* = 0.048$ nm. It is observed (see Figure 1.20b) that the data of $E_\eta(\eta_0)$ for water and aqueous ammonium oxalate solutions of various concentrations follow the same linear dependence (1.52). This observation suggests that the critical

volume V^* and the corresponding radius r^* are associated with the structure of the solvent water.

The estimated value of the hole radius r^0 is approximately four times the average radius $r_{\text{H}_2\text{O}} = 0.138$ nm of water molecules. This conclusion is consistent with relation (1.50), which predicts that the average radius $r_{\text{H}_2\text{O}}$ of holes participating in viscous flow is greater than 0.168 nm. The value of the critical radius r^* is approximately twice the maximum displacement δ_{max} of a solvent molecule from its equilibrium position due to the thermal energy, i.e.

$$\delta_{\text{max}} = \left(\frac{2k_{\text{B}}T}{f} \right)^{1/2} \approx 0.022 \text{ nm}, \quad (1.53)$$

where $k_{\text{B}}T$ is the thermal energy of water molecules at its melting point T_{m} and $f \approx 15$ N/m is the force constant of ice lattice.

From the above discussion it follows that the value of the new temperature T^* is close to the melting point of ice, whereas the value of the critical radius r^* is related to the thermal vibrations of solvent molecules. Thus, it may be concluded that the values of the constants A_1 and B_1 of Eq. (1.52) are determined by the properties of solvent. In contrast to this, r^0 and r are the radii of holes in the solvent and the solution, respectively, and are associated with the viscous flow.

Finally, it should be emphasized that the values of the activation energies ΔG^0 and F for viscous flow of solvents and solutions decrease with increasing temperature. This is due to the fact that water and aqueous solutions behave as associated liquids with network structure. In associated liquids, the activation energy E_{η} for viscous flow is determined by the energy required to break the bonds of the network, whereas the fraction of the broken bonds increases with temperature (Bockris and Reddy, 1970).

1.5 Saturated Solutions

Saturated solutions are inherited by changes in solute concentration dissolved in suitable solvents with an increase in temperature. Therefore, a reasonable representation of the properties of saturated solutions by mathematical expressions is possible only through their dependence on temperature. In the case of solutions containing not very high solute concentrations, their properties such as density and viscosity increase practically linearly with solute concentration (see Section 1.4). However, for real solutions, the temperature dependence of the solubility of a solute in a given solvent is usually given by polynomial and Arrhenius-type relations (see Section 2.4). By combining these relationships with the linear dependence of solute concentration, one obtains equations similar to Eqs. (1.12), (1.13), and (1.17). In the case of density d , one obtains

$$d = d_0^* + a_1^*(T - T_0) + a_2^*(T - T_0)^2, \quad (1.54)$$

and

$$d = d_0^{**} \exp[\beta_0^*(T - T_c)^2]. \quad (1.55)$$

In Eq. (1.54), d_0^* , a_1^* , and a_2^* are new constants and d_0^* is the saturated solution density at T_0 , whereas in Eq. (1.55), d_0^{**} and β_0^* are new constants and d_0^{**} is the density corresponding to T_c . Note that for saturated solutions $d^* > d_0$, $a_1^* > a_1$, and $a_2^* > a_2$. In the case of viscosity η , Eq. (1.44), which includes solution concentration, may be used. This relation predicts that an increase in solute concentration in the solution leads to an increase in the activation E_η and a decrease in the preexponential factor η_0 . Some examples illustrating the validity of the above predictions are given below.

Figure 1.17a shows the dependence of the density d of saturated aqueous solutions of potassium bichromate (chemical formula $K_2Cr_2O_7$; abbreviation K bichromate or KBC) and sodium and ammonium oxalates on their temperature T according to Eq. (1.54), whereas Figure 1.17b presents the data as $\ln \phi_V = -\ln d$ of the above $d(T)$ data for saturated solutions against $(T - T_c)^2$ according to Eq. (1.55). The best-fit values of the plots are listed in Table 1.9, where the corresponding fitting parameters for water are also included for comparison.

From Table 1.9 and Figure 1.17, it may be seen that only saturated Na_2Ox solutions show a trend similar to that of water. As in water, here both a_1^* and a_2^* are negative but the value of d_0^* increased. In contrast to the behavior of Na_2Ox solutions, for KBC and Am_2Ox saturated solutions, not only the values of the d_0^* are increased but also the values of the constants a_1^* and a_2^* are positive and their values for KBC solutions are much higher than those for Am_2Ox solutions. Similarly, one notes from Table 1.9 that the specific volume $\phi_{V0} \approx 1/d_0^*$ for KBC solutions is lower than that for Am_2Ox solutions but the parameter β^*/T_c^2 for different solute solutions is more informative. As in the case of water, this β^*/T_c^2 parameter is negative for Na_2Ox solutions but is positive for KBC and Am_2Ox solutions and its value is much higher for KBC solutions than that of Am_2Ox solutions. These different trends of saturated solutions of different salts are associated with the differences in their solubilities in water with temperature and the solvation of solute ions.

Figure 1.18a and b shows typical examples of the dependence of the viscosity η of aqueous saturated solutions of potassium bichromate and sodium and ammonium oxalates, and three disaccharides on their temperature saturation T , respectively. Two different trends of the viscosity data are obvious. In the case of KBC, Am_2Ox , Na_2Ox , and sucrose, the viscosity η decreases with increasing saturation temperature of the solution, but an opposite trend of an increase in the viscosity η of the saturated solutions with increasing temperature of two other disaccharides (i.e. trehalose and maltitol) is observed. These different

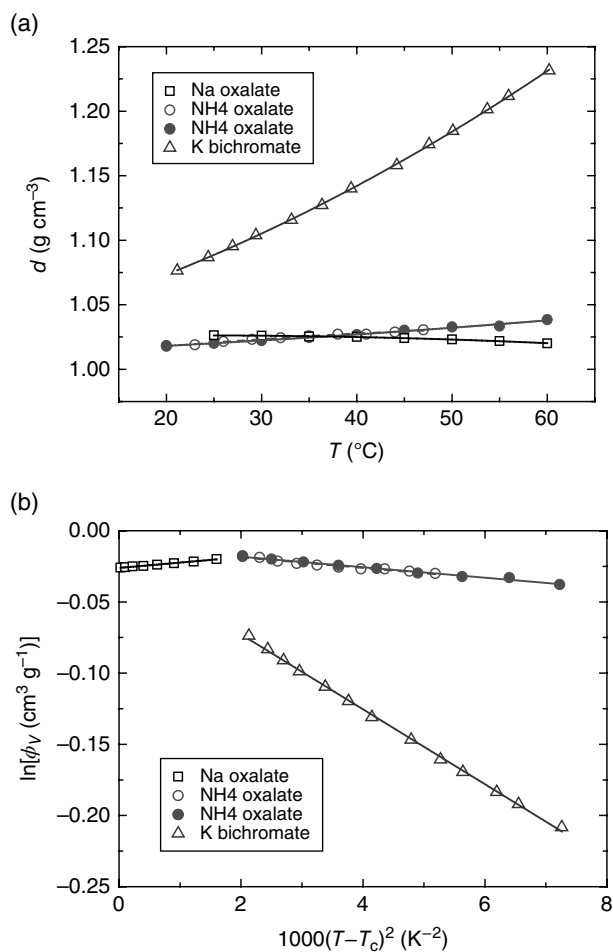


Figure 1.17 (a) Dependence of density d of saturated aqueous solutions of sodium and ammonium oxalates and potassium bichromate on their temperature T . (b) Plots of $\ln\phi_V$ of above saturated solutions against $(T - T_c)^2$ according to Eq. (1.13). Original data for sodium oxalate, ammonium oxalate, and potassium bichromate solutions are from Misztal (2004), Frej et al. (1998, 2000), and Szewczyk et al. (1985), respectively. *Source:* Data shown by open and filled circles for ammonium oxalate from Frej et al. (2000) and (1998), respectively.

trends of the temperature dependence of viscosity of saturation solutions are associated with the opposite effects of solution temperature and solute concentration (Gharsallaoui et al., 2008):

- 1) As is the usual situation, at a particular temperature the viscosity increases with increasing solute concentration.

Table 1.9 Constants of Eqs. (1.54) and (1.55) for aqueous saturated solutions.

Salt	Eq. (1.54)			Eq. (1.55)			
	$d_0^*(\text{g}\cdot\text{cm}^{-3})$	$10^{-3}a_1^*(\text{g}\cdot\text{cm}^{-3}\cdot\text{K})$	$10^{-5}a_2^*(\text{g}\cdot\text{cm}^{-3}\cdot\text{K}^2)$	$-10^{-2}\ln\phi_{V0}^{**}$	$-10^{-6}\beta_0^*(\text{K}^{-2})$	T_c (K)	$10^{-11}\beta^*/T_c^2$ (-)
Water	1.00165	-0.129	-2.8247	0.356	-2.76	298	-3.10
KBC	1.0249	1.92	2.535	2.017	26.3	298	29.5
Na2Ox	1.0238	-0.210	-0.448	2.61	-3.74	253	-5.83
Am2Ox ^a	1.0114	0.286	0.259	1.120 dashed	0.373	298	4.19
Am2Ox ^b	1.0023	0.904	-0.674	1.087 solid	0.368	298	4.13

^a Open circles and dashed line.^b Filled circles and solid line.

- 2) For the solution of a given solute concentration, the viscosity decreases with increasing solution temperature.

When factor (2) of the effect of temperature dominates factor (1) of solute concentration, the viscosity of the saturated solutions decreases with increasing temperature. This is the situation in the case of aqueous saturated solutions of KBC, Am2Ox, Na2Ox, and sucrose. Here, solute–solute interactions are stronger than solute–solvent interactions. However, when factor (1) of solute concentration dominates factor (2) of solution temperature, the saturated solution viscosity increases with increasing temperature. This is the situation for aqueous saturated solutions of maltitol and trehalose. In this case, solute–solvent interactions are stronger than solute–solute interactions.

The $\eta(T)$ data for the saturated solutions of different salts and disaccharides may be described reasonably well by a quadratic equation but the values of the parameters of the quadratic equation are not informative. Therefore, the $\eta(T)$ data for the saturated solutions of different solutes were analyzed using Eq. (1.44). Figure 1.19a and b shows the dependence of $\ln\eta$ of aqueous saturated solutions of potassium bichromate and sodium and ammonium oxalates, and of three disaccharides, respectively, on $1/T$, with the plots obtained with the best-fit parameters listed in Table 1.10. Values of E_η for concentrated aqueous solutions of the compounds are given in the parentheses in the last column.

The data of η_0 and E_η for aqueous saturated solutions follow relation (1.52), as shown in Figure 1.20a. However, the $E_\eta(\eta_0)$ data for saturated solutions of disaccharides and salts lie on two separate linear plots with the constants: $A_1 = 1550.6 \pm 218.2 \text{ K}$ and $B_1 = 352.1 \pm 21.5 \text{ K}$, and $A_1 = 86.2 \pm 14.1 \text{ K}$ and $B_1 = 314.3 \pm 2.9 \text{ K}$, and new preexponential factors $A_1/B_1 = \ln\eta_0^* = 4.4044$ or $\eta_0^* = 81.81 \text{ mPa}\cdot\text{s}$ and $A_1/B_1 = \ln\eta_0^* = -0.27434$ or $\eta_0^* = 0.760 \text{ mPa}\cdot\text{s}$,

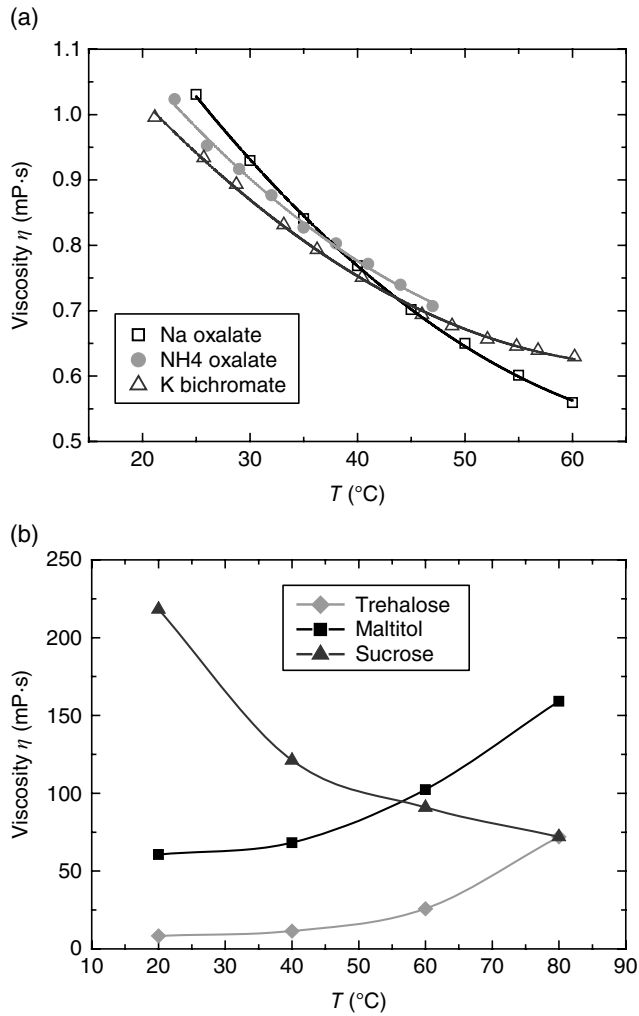


Figure 1.18 Dependence of viscosity η of aqueous saturated solutions of (a) sodium and ammonium oxalates and potassium bichromate, and (b) three disaccharides on their temperature saturation T . *Source:* Original data in (a) for sodium oxalate, ammonium oxalate, and potassium bichromate solutions are from Misztal (2004), Frej et al. (2000), and Szweczyk et al. (1985), respectively, but in (b) for disaccharides are from Gharsallaoui et al. (2008).

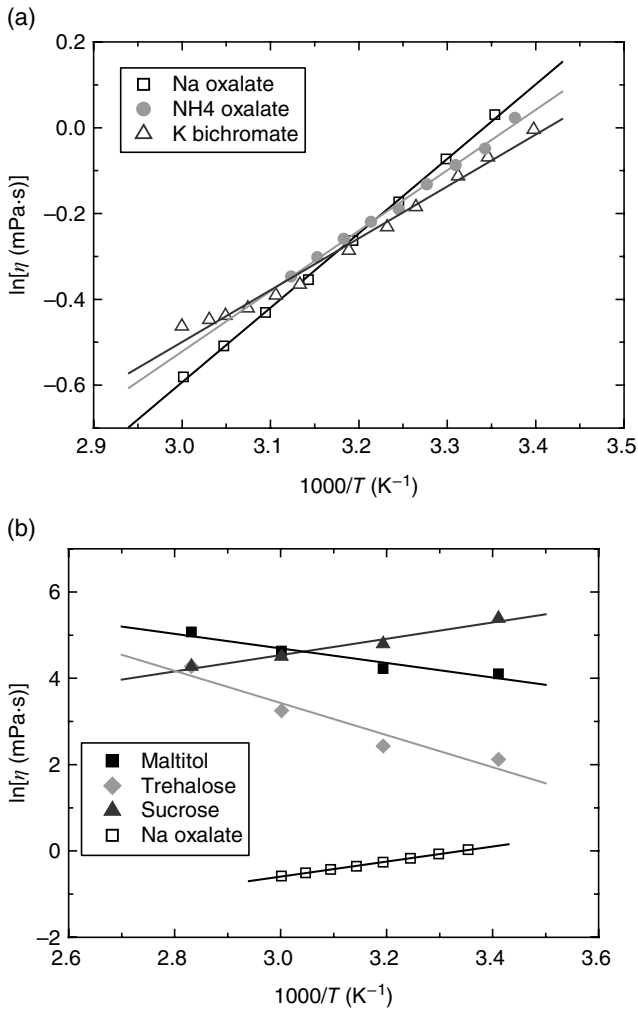


Figure 1.19 Dependence of $\ln\eta$ of aqueous solutions of (a) sodium and ammonium oxalates and potassium bichromate, and (b) three disaccharides on $1/T$. Source: Original data is shown in Figure 1.18a and b, respectively.

respectively. As shown in Figure 1.20b, these linear dependences are similar to those observed for the data of η_0 and E_η for aqueous ammonium oxalate solutions of different concentrations. Differences in the $E_\eta(\eta_0)$ plots of these oxalate solutions and saturated aqueous solutions of different salts are clearly seen. The main effect of saturation of the solution is to increase the value of E_η of a compound.

Table 1.10 Values of constants of Eq. (1.16) for saturated solutions.

Solvent	T_m (K)	$-\ln\eta_0$	$10^3 E_\eta/R_G$ (K ⁻¹)	η_0 (mPa·s)	E_η (kJ·mol ⁻¹)	$E_\eta/R_G T_m$ (-) ^a
Water	273.15	6.3108	1.86078	$1.817 \cdot 10^{-3}$	15.47	6.81
K ₂ Cr ₂ O ₇	671.15	4.1253	1.20858	$1.616 \cdot 10^{-2}$	10.04	4.42 (1.62)
Na ₂ C ₂ O ₄	523.15	5.7986	1.73516	$3.032 \cdot 10^{-3}$	14.43	6.35 (3.31)
(NH ₄) ₂ C ₂ O ₄	406.15	4.7458	1.40807	$8.688 \cdot 10^{-3}$	11.71	5.15 (3.47)
Sucrose	459.15	1.1342	1.88985	0.322	15.71	6.92 (4.11)
Maltitol	419.15	-9.7409	-1.68356	$1.70 \cdot 10^4$	-14.0	-6.16 (-4.02)
Trehalose	488.15	-14.57556	-3.7159	$2.14 \cdot 10^6$	-30.90	-13.60 (-7.61)

^a Values in parentheses refer to concentrated solutions.

The above values of η_0^* give the following threshold volumes $V^* = 8.1 \cdot 10^{-33}$ and $8.718 \cdot 10^{-31} \text{ m}^3$, and the threshold radii $r^* = 0.012$ and 0.059 nm for aqueous saturated solutions of disaccharides and salts, respectively. In comparison with the value of the threshold radius $r^* = 0.048 \text{ nm}$ for aqueous ammonium oxalate solutions of various concentrations, mentioned above, the value of this radius r^* for aqueous saturated solution of different salts is somewhat increased but that for disaccharide solutions is decreased enormously. These opposite effects of salts and disaccharides are due to their chemical nature. Moreover, as judged from the ratio $E_\eta/R_G T_m$ (with $T_m = 273.15 \text{ K}$ for water), aqueous solutions of salts and sucrose behave as associated systems, but this trend of associated systems is somewhat disrupted in aqueous potassium bichromate and ammonium oxalate solutions and is strongly disrupted in aqueous maltitol and trehalose solutions.

Crystallization always occurs in supersaturated solutions and occurs as a result of integration of entities present in them. Therefore, it is interesting to estimate the size of these entities from the data of viscosity of saturated solutions and supersaturated solutions. For this purpose, as an example, we use the viscosity data of concentrated ammonium oxalate solutions in the temperature range between 291.15 and 320.15 K and saturation concentrations c from 0.36 to 0.75 mol·dm⁻³ (Frej et al., 2000). Viscosity measurements were made for each saturated solution of concentration c_s starting from a temperature of 5 K above the saturation temperature T_s (undersaturation range) to the temperature T_N of onset of nucleation (supersaturation range). For constant selected temperatures T_N corresponding to known initial saturation concentrations c_s , viscosity data for supersaturated solutions of other c_s were considered for the analysis. Viscosity data for different c_s were also analyzed.

Figure 1.21 presents the dependence of relative viscosity η/η^0 of aqueous supersaturated and saturated solutions of ammonium oxalates on the original

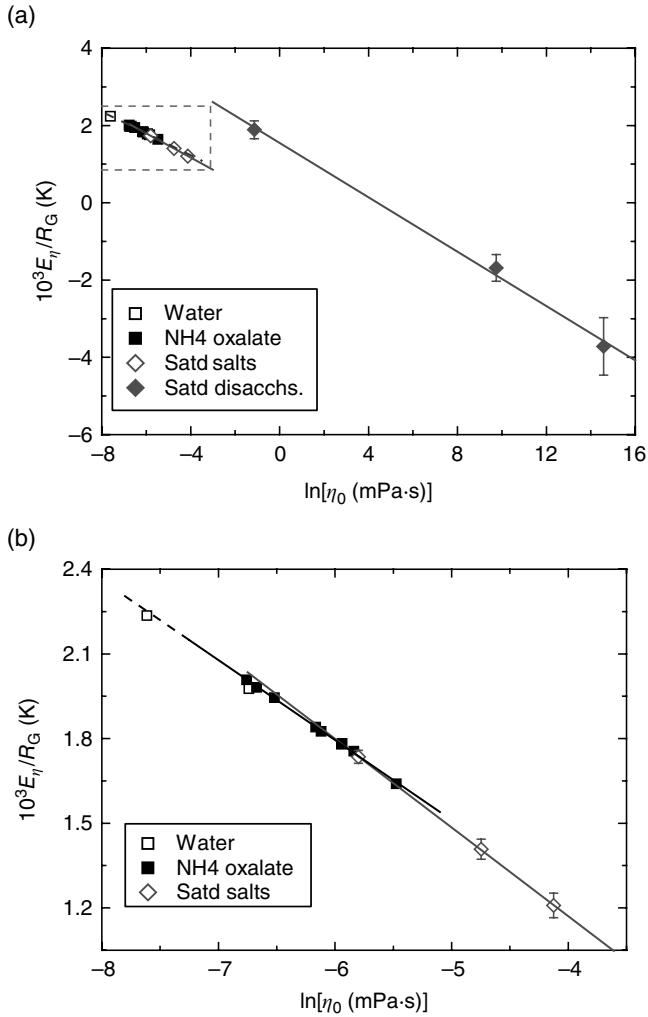


Figure 1.20 Plot of E_n/R_G against $\ln\eta_0$ for aqueous saturated solutions of different compounds and aqueous ammonium oxalate solutions of different concentrations according to Eq. (1.52). In (b) details of data of rectangular area. Former and latter data are from Table 1.10 and Figure 1.16.

saturation concentration c_s . Here, η^0 is the viscosity of water. Supersaturated solutions corresponding to different T_N are represented by different symbols, whereas saturated solutions are shown by asterisks. The data for supersaturated solutions were fitted according to Einstein's relation (1.37). The solid curve represents the data with an effective concentration $c_s(\text{eff}) = c_s - c_s^*$, where

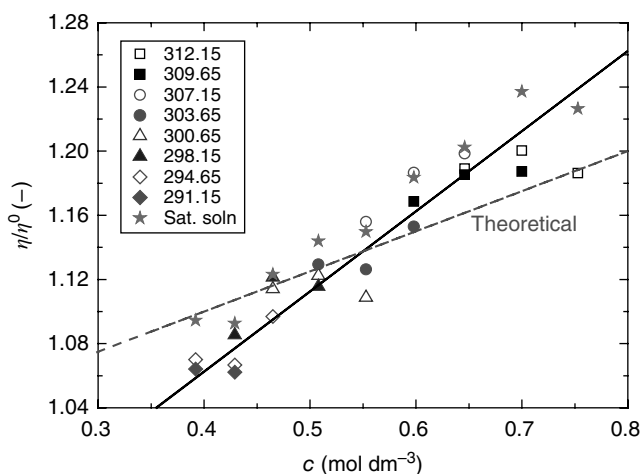


Figure 1.21 Dependence of relative viscosity η/η^0 of aqueous supersaturated and saturated solutions of ammonium oxalates on the original concentration c . Supersaturated solutions are represented by different symbols with saturation temperature given in K in the inset, whereas saturated solutions are shown by asterisks. *Source:* Original data from Frej et al. (2000). See text for details.

$c_s^* = 0.275 \text{ mol}\cdot\text{dm}^{-3}$ is a threshold concentration beyond which relation (1.37) applies and has slope $0.5 \text{ dm}^3\cdot\text{mol}^{-1}$. The data for saturated solutions also have a similar slope with a lower threshold of about $0.2 \text{ mol}\cdot\text{dm}^{-3}$. However, in the entire concentration range the data may be described with a slope $0.25 \text{ dm}^3\cdot\text{mol}^{-1}$ (dashed curve). These slopes give $\phi = 0.2$ and $0.1 \text{ dm}^3\cdot\text{mol}^{-1}$, from which one obtains the radius $r = 0.43$ and 0.34 nm of entities participating in viscous flow. These values are somewhat lower than the value given in Table 1.8 but are about twice larger than the crystallographic radii of 0.148 and 0.2 nm of individual NH_4^+ and $\text{C}_2\text{O}_4^{2-}$ ions, respectively. These results suggest that entities participating in crystallization from solution are solvated ions.

1.6 High-Temperature Solvents and Solutions

Some properties of solutions of ionic salts and molecular compounds dissolved in solvent water were described in the preceding sections. The role of the solvent here is to overcome forces between ions/molecules in the crystal to produce mobile entities in the form of ions/molecules in their solution by solvation processes. The solvent used here is in the liquid state at normal temperature and pressure conditions. Therefore, in the crystallization literature

such solvents and solutions are frequently referred to as low-temperature solvents and solutions.

There is another method of overcoming forces between ions/molecules in a crystal by heating it. The heat energy supplied to the solid increases the extent of vibrations of its ions/molecules until thermal forces prevail over long-range order leading to the melting of the solid. The molten material now has plentiful free space for the ceaseless motion of ions/molecules. Such molten liquids of particular materials dissolve other materials forming homogeneous solutions at high temperatures. In the crystallization literature the molten liquids obtained by heating materials, which are in the solid state under ordinary temperature and pressure conditions, and their homogeneous mixtures with other materials are called high-temperature solvents and solutions, respectively. High-temperature solvents are usually referred to as fluxes and, depending on the material to be crystallized, their composition may be quite complex.

Composition of the components of a flux determines not only its various properties but also the solubility of a substance in it and is associated with the formation of ions and complexes (Görnert and Sinn, 1985; Görnert and Voigt, 1984; Wanklyn, 1983). Volatility and viscosity of fluxes and solutions are important issues in high-temperature crystallization and it is frequently found that less viscous solutions are more volatile (Pritula and Sangwal, 2015). As in the case of different low-temperature solutions and solvents, the viscosity of high-temperature solutions decreases with an increase in temperature and follows Arrhenius-type relation (1.16). Values of best-fit parameters $\ln \eta_0$ and E_η/R_G for some systems are given in Table 1.11.

As in the case of aqueous saturated solutions of different compounds and aqueous ammonium oxalate solutions of different concentrations (see Figure 1.20), the data of E_η/R_G against $\ln \eta_0$ for these high-temperature systems also follows Eq. (1.52), as shown in Figure 1.22 with constants $A_1 = 4424 \pm 202$ K and $B_1 = 1404 \pm 34$ K, and new preexponential factor $A_1/B_1 = \ln \eta_0^* = 3.15$ or $\eta_0^* = 23.34$ mPa·s. This value of η_0^* gives the following threshold volume $V^* = 2.84 \cdot 10^{-33}$ m³ and the threshold radius $r^* = 0.019$ nm. This value is comparable with the value of the maximum displacement δ_{\max} of a solvent molecule from its equilibrium position due to the thermal energy (see Eq. (1.53)).

Taking the melting temperature $T_m = 722$ K for K_8 solution representative of all solutions, the values of $E_\eta/R_G T_m$ were calculated using the data of E_η/R_G given in Table 1.11. It may be observed that the ratio $E_\eta/R_G T_m = 4.47$ for the solution used for the growth of $KLu(WO_4)_2$ crystals but its value exceeds 10 for the remaining solutions used for the growth of $KTiOPO_4$ and $CsLiB_6O_{11}$ crystals. This suggests that crystal growth from high-temperature solutions mainly occurs in associated solutions. The low value of the threshold radius r^* obtained above is connected with the associated nature of the solutions.

Table 1.11 Calculated values of parameters of Eq. (1.17) for some growth solutions.

Crystal ^a	Solution ^b	$-\ln \eta_0$	$10^3 E_f / R_G$ (K)	η_0 (mPa·s)	E_f (kJ·mol ⁻¹)
KTP	K ₈	3.65 ± 0.35	9.89 ± 0.42	2.6·10 ⁻²	82.2 ± 3.5
	K ₈ + BaF ₂	4.28 ± 0.25	10.34 ± 0.30	1.4·10 ⁻²	86.0 ± 2.5
CLBO	Cs ₂ CO ₃ : Li ₂ CO ₃ : H ₃ BO ₃ (1 : 1 : 11)	11.77 ± 1.11	21.20 ± 1.26	7.7·10 ⁻⁶	176.3 ± 10.5
	Cs ₂ CO ₃ : Li ₂ CO ₃ : H ₃ BO ₃ (1 : 1 : 12)	10.40 ± 0.90	19.48 ± 1.02	3.0·10 ⁻⁵	162.0 ± 8.5
	Cs ₂ CO ₃ : Li ₂ CO ₃ : H ₃ BO ₃ : NaF (1 : 1 : 12 : 0.5)	9.22 ± 0.73	17.79 ± 0.83	9.9·10 ⁻⁵	147.9 ± 6.9
	Cs ₂ CO ₃ : Li ₂ CO ₃ : H ₃ BO ₃ : NaF (1 : 1 : 12 : 0.67)	9.69 ± 0.84	18.22 ± 0.95	6.2·10 ⁻⁵	151.5 ± 7.9
KLu(WO ₄) ₂	Cs ₂ CO ₃ : Li ₂ CO ₃ : H ₃ BO ₃ : NaF (1 : 1 : 12 : 2)	9.07 ± 0.47	16.69 ± 0.53	1.2·10 ⁻⁴	138.3 ± 4.4
	KLu(WO ₄) ₂ : K ₂ W ₂ O ₇ (12 : 88)	0.68 ± 0.38	3.37 ± 0.48	1.96	28.0 ± 4.0

Source: Adapted from Pritula and Sangwal (2015).

^a KTB – KTiOPO₄, CLBO – CsLiB₆O₁₁.

^b K₈ (K₈P₆O₁₉).

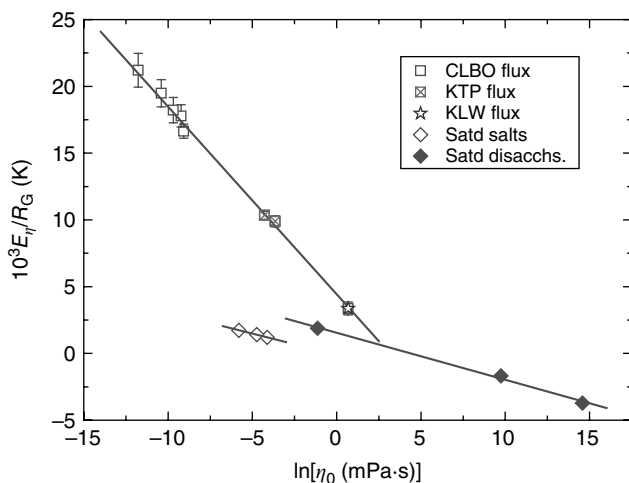


Figure 1.22 Linear relationship between E_n/R_G and $\ln\eta_0$ for some high-temperature systems according to Eq. (1.52). Data of E_n/R_G against $\ln\eta_0$ for aqueous saturated solutions of different compounds and aqueous ammonium oxalate solutions of different concentrations are also shown in the figure.

References

- Asadi, M. (2006). *Beet-Sugar Handbook*. Hoboken, NJ: Wiley. Table A12.
- Atkins, P.W. (1998). *Physical Chemistry*, 6e. Oxford: Oxford University Press.
- Bockris, J.O.'M. and Reddy, A.K.N. (1970). *Modern Electrochemistry*, vol. 1. New York: Plenum Press. Chap. 2.
- Eggers, D.F., Gregory, N.W., Halsey, G.D., and Rabinovitch, B.S. (1964). *Physical Chemistry*. New York: Wiley.
- Feakins, D., Freemantle, D.J., and Lawrence, K.G. (1974). Transition state treatment of the relative viscosity of electrolytic solutions. Applications to aqueous, non-aqueous and methanol + water systems. *J. Chem. Soc. Faraday Trans.* 70: 795–806.
- Feakins, D.F.M.B., Waghorne, W.E., and Lawrence, K.G. (1993). Relative viscosities and quasi-thermodynamics of solutions of tert-butyl alcohol in the methanol-water system: a different view of the alkyl-water interaction. *J. Chem. Soc. Faraday Trans.* 89: 3381–3389.
- Frej, H., Jakubczyk, M., and Sangwal, K. (1998). Density, surface tension, and refractive index of aqueous ammonium oxalate solutions from 293 K to 333 K. *J. Chem. Eng. Data* 43: 415–418.
- Frej, H., Balińska, A., and Jakubczyk, M. (2000). Density and viscosity of undersaturated, saturated, and supersaturated aqueous ammonium oxalate solutions from 287 K to 325 K. *J. Chem. Eng. Data* 45: 415–418.

- Gharsallaoui, A., Rogé, B., and Mathlouthi, M. (2008). Water-disaccharides interactions in saturated solution and the crystallisation conditions. *Food Chem.* 106: 1329–1339.
- Goldsack, D.E. and Franchetto, R.C. (1977). The viscosity of concentrated electrolyte solutions. I. Concentration dependence at fixed temperature. *Can. J. Chem.* 55: 1062–1072.
- Goldsack, D.E. and Franchetto, R.C. (1978). The viscosity of concentrated electrolyte solutions. II. Temperature dependence. *Can. J. Chem.* 56: 1442–1450.
- Görner, P. and Sinn, E. (1985). Fundamental aspects of flux growth. In: *Crystal Growth of Electronic Materials* (ed. E. Kaldis), 23–39. Amsterdam: Elsevier.
- Görner, P. and Voigt, F. (1984). High temperature solution growth of garnets: theoretical models and experimental results. In: *Current Topics in Materials Science*, vol. 11 (ed. E. Kaldis), 1–149. Amsterdam: North-Holland.
- Horvath, A.L. (1985). *Handbook of Aqueous Electrolyte Solutions: Physical Properties, Estimation and Correlation Methods*. Chichester: Ellis Horwood. Chap. 2.
- Lide, D.R. (1996/1997). *Handbook of Chemistry and Physics*, 77e. Boca Raton, FL: CRC Press.
- Misztal, R. (2004). Badanie własności fizykochemicznych roztworów wodnych szczawianu sodu w obecności domieszek (Study of physico-chemical properties of aqueous sodium oxalate solutions in the presence of impurities). PhD thesis. Jagiellonian University, Kraków.
- Mortimore, R.G. (2008). *Physical Chemistry*, 3e. Amsterdam: Elsevier. Chap. 23.
- Pritula, I. and Sangwal, K. (2015). Fundamentals of crystal growth from solutions. In: *Handbook of Crystal Growth*, vol. II (ed. T. Nishinaga and P. Rudolph), 1185–1227. Elsevier.
- Sangwal, K. (1987). A new equation for the temperature dependence of density of saturated aqueous solutions of electrolytes. *Cryst. Res. Technol.* 22: 789–792.
- Sangwal, K. (1989). On the estimation of surface entropy factor, interfacial-tension, dissolution enthalpy and metastable zone-width for substances crystallizing from solution. *J. Cryst. Growth* 97: 393–405.
- Sangwal, K., Frej, H., and Misztal, R. (2004). On the dimensions of species participating in the growth of ammonium oxalate monohydrate crystals from viscosity data of concentrated aqueous solutions. *Cryst. Res. Technol.* 39: 705–711.
- Stokes, R.H. and Mills, R. (1965). *Viscosity of Electrolytes and Related Properties*. Oxford: Pergamon Press.
- Szewczyk, J. and Sangwal, K. (1988). Density, refractive index, and specific refraction of aqueous lithium iodate solutions. *J. Chem. Eng. Data* 33: 418–423.
- Szewczyk, J., Sokołowski, W., and Sangwal, K. (1985). Some physical properties of saturated, supersaturated, and undersaturated aqueous potassium bichromate solutions. *J. Chem. Eng. Data* 30: 243–246.
- Wanklyn, B. (1983). The present status of flux growth. *J. Cryst. Growth* 65: 533–540.
- Wright, M.R. (2007). *An Introduction to Electrolyte Solutions*. Chichester: Wiley.

